Spatial redistribution of a flux of charged particles in a crystal lattice

M. A. Kumakhov

Nuclear Physics Research Institute of the Moscow State University
Usp. Fiz. Nauk **115**, 427–464 (March 1975)

A review is given of the problem of passage of charged particles through a crystal lattice and determination of the location of foreign atoms inside the unit cell. Chapter 1 is introductory. Chapter 2 considers the effect of spatial redistribution of the flux of charged particles in axial channeling. The effect of multiple scattering on the flux at both large and small depths is discussed. A relation is demonstrated between the location of the foreign atoms and the location of the peaks in the angular distribution. Chapter 3 considers the redistribution of the flux and multiple scattering in planar channeling. Chapter 4 is devoted to channeling of heavy ions. A technique is presented for calculation of the spatial redistribution of implanted ions with inclusion of the channeling effect. Chapter 5 presents a review of experiments on determination of the location of foreign atoms inside the unit cell.

PACS numbers: 61.80.M, 61.80.P

CONTENTS

1. INTRODUCTION

Experiments carried out in the last ten to fifteen years have revealed a number of special features of the interaction of charged particles with a crystal lattice. The order of the lattice leads to orientation effects.

The first of these apparently was observed by Bredov and co-workers[1] and by Davies et al.[2], who found anomalously long ranges of ions with energies of several keV in crystalline targets. To determine the ranges of the ions, Bredov et al. used the tracer method. They were able to show that the anomalous penetration effect is due not to diffusion but to the initial kinetic energy of the ions.

A somewhat different effect was observed by Wehner[3], who discovered an anisotropy in the sputtering of single-crystal targets bombarded by heavy ions. The first interpretation of this effect was given by Silsbee[4] (the theory of focusing of atomic collisions in crystals).

Rol and co-workers[5] and Molchanov and Tel'kovskiĭ[6] established the existence of a sharp dependence of the yield of sputtered atoms on the angle of incidence of the ions on a single crystal. Mashkova et al.[7] also established that the coefficient of ion-electron emission varies rapidly when the ion beam travels along a close-packed row of atoms. A theory of these phenomena was proposed by Odintsov[8] and Martynenko[9].

Somewhat later Robinson and Oen[10] directly modeled the ion penetration process in a copper lattice by computer and reached the conclusion that an ion whose trajectory in the crystal passes at a small angle to a direction of close packing of atoms has a significantly greater range than for a random direction. Robinson and Oen named this phenomenon channeling.

Several groups of experimenters independently confirmed the existence of channeling.[11-13] The experiments of Bredov et al.[1] and Davies et al.[2] Obviously have a direct relation to channeling.

Another effect, the so-called shadow or blocking effect, was observed and studied by Domeij and Björkvist[14], Tulinov and co-workers[15], and Hemmel and Holland[16]. In these studies it was shown that because of the order of the lattice the emission of charged particles from a crystal along atomic rows and planes becomes impossible, as a consequence of which shadows of the atomic rows and planes appear on photographic plates recording the intensity of particle emission. A calculation of the shape of the shadow for a Firsov potential was carried out by Martynenko[9]. Agranovich et al.[17] calculated the shadow with inclusion of the thermal vibrations of the atoms. Tulinov[15] calculated the shadow with inclusion of nuclear screening by electrons.

The basic concepts of the theory of the channel effect and blocking were formulated by Lindhard.[18,19] He introduced the idea of atomic strings and planes and replaced the potentials of the individual atoms by the potentials of continuous atomic strings and planes. Lindhard was able to obtain the value of the critical angle ψ_1 within which channeling can be observed. A statistical description is used in calculation of the specific parameters in Lindhard's theory.

For heavy particles (protons, α particles, and heavier ions) the classical theory of Lindhard turns out to be completely satisfactory.[21] It provides the possibility of explaining any of the experiments carried out up to the present time. However, for a description of the channeling of light particles, electrons and posi-

trons, a quantum-mechanical discussion is apparently necessary in many cases.

Kagan and Kononets[20] utilized the density matrix method to describe channeling and obtained the dependence of the Rutherford-scattering yield on the angle of incidence.

Subsequently, inelastic processes were taken into account in the theory. It turned out that at depths >1000 Å the nondiagonal terms of the density matrix disappear and the motion of the ions in the channel can be described by an equation of the Boltzmann type. The theory predicts diffraction effects near the crystal surface. In terms of this formalism, in particular, it is possible to calculate the dechanneling function and the energy spectrum. This approach is convenient in that it permits the distribution of the particles over the cross section of the channel to be obtained.

The quantum-mechanical theory[20] is now apparently very rigorous and complete.

Scattering in a thin crystal from the quantum-mechanical point of view has been studied by Kalashnikov, Ryazanov, Koptelov, and Chukhovskiĭ.[22]

With allowance for the screening of neighboring nuclei by an atomic string, they were able to obtain an expression for the differential cross section for elastic scattering.

The interrelation of the quantum and classical approaches was investigated by Newton and Chadderton.[23] They assume that the quantum approach should be diffractive, since it is necessary to consider a plane wave at the entrance to the crystal and a set of Bloch waves inside it. For more detail on this question see the articles by Chadderton[121].

In recent years the orientation effects have been used in a large number of experiments[24,25] to study the dynamics of radiation damage of crystals, to determine the location of impurity atoms, and also in atomic and nuclear physics. The channeling of ions is accompanied by a new physical phenomenon—the effect of spatial redistribution of the flux of charged particles in a crystal lattice. The present article is devoted to study of this effect and the possibilities of its utilization in physics.

2. SPATIAL REDISTRIBUTION OF THE CHARGED-PARTICLE FLUX IN AXIAL CHANNELING

a) Main assumptions used in interpretation of experiments determining the location of foreign atoms. When a beam of ions hits a crystal parallel to any crystallographic axis, the beam is separated into two components: channeled and random, i.e., unchanneled. The channeled ions do not approach a string of atoms closer than some distance r_{min}. According to Lindhard, $r_{min}^2 = u_\perp^2 + a^2$, where $u_\perp$ is the amplitude of thermal vibrations of the atom perpendicular to the string considered; a is the screening parameter. The fraction of atoms which does not enter the channel is $\pi r_{min}^2 Nd$, where Nd is the number of chains per cm^2 of surface perpendicular to the ion beam direction; N is the concentration of atoms per cm^3; d is the distance between atoms in a string.

Most physical processes such as Rutherford scattering at large angles, nuclear reactions, production of characteristic x rays from inner atomic shells, and so forth require small impact parameters, at least less than r_{min}. In order of magnitude $r_{min} \sim 0.1$ Å, and all processes require impact parameters one to two orders of magnitude smaller. The use of channeling to determine the location of a foreign atom is based on just this fact.

Let us consider, for example, the case of Rutherford scattering. First a combardment of an unoriented target is carried out. During a certain length of time the detector records the number of particles scattered into some solid angle determined by the location of the detector relative to the target and the angular resolution of the detector. In this case those particles are detected which are scattered by the foreign atoms and not by lattice atoms. This can always be done if the mass of the foreign atom is greater than the mass of the lattice atom, since in this case the energy of particles scattered by the foreign atoms is higher than that of particles scattered by the lattice atoms. Therefore by adjusting the detector to a definite energy interval it is possible to discriminate against particles scattered by the lattice atoms. If the mass of the foreign atom is less than the mass of the lattice atom, this becomes difficult since there will be a background from scattering from lattice atoms. In this case it is possible to record for a certain location of the foreign atom not the scattered particles but nuclear reaction products.

After the bombardment of the unoriented target is carried out, the beam is directed along some channel and in a certain time the number of particles at the detector is measured.

If the foreign atoms are in substitutional states or inside the region r_{min}, the ratio of the number of particles detected in channeling to the number of particles detected for unoriented bombardment is roughly equal to $y_{ch}/y_n \approx \pi r_{min}^2 Nd$, i.e., roughly equal to the fraction of ions not entering the channel at the beginning. Typical values are $y_{ch}/y_n \approx -5 \times 10^{-2}$, i.e. several percent. Thus, if the foreign atoms are localized inside the region r_{min}, a strong reduction of the yield is obtained for channeling, roughly by two orders of magnitude, in comparison with the case of bombardment of an unoriented target. The foreign atoms, for example, in Si and Ge cannot occupy tetrahedral interstitial positions. Along the rows ⟨111⟩ and ⟨100⟩ these interstitial positions are blocked by the atoms, and along the ⟨110⟩ row they are outside the region r_{min}. This fact is utilized in interpretation of the experiments. If the foreign atoms are outside the region r_{min}, i.e., in a region accessible to the channeled ions (or in other words in interstitial positions), it is assumed that in this case there should not be a decrease in the yield of particles for channeling, i.e., here $y_{ch}/y_n = 1$. This last assumption implicitly supposes that the flux of ions in the channel is uniform, i.e., the same as on entry into the channel at the surface.

This assumption of uniformity of the ion flux in the channel is fundamental and has been used in interpretation of the experiments carried out in 1966—1970 (see for example refs. 24—26). In these experiments, naturally, there was generally no consideration of the possibility of determining the location of a foreign atom located in an interstitial position beyond the region r_{min}. In fact, if the flux in the channel is uniform, the number of particles recorded in the detector will be

constant, independent of just what interstitial position the atom is located in, under identical conditions.

Our work is mainly devoted to investigation of the distribution of the flux of channeled ions. As we will see below, the main assumption which has been used in interpretation of the experiments, namely, the assumption of uniformity of the ion flux in the channel, has turned out to be incorrect. As a consequence, the quantitative, and in a number of cases also the quantitative interpretation of these experiments has turned out to be wrong.

There is, however, another significantly more important conclusion. As a consequence of the fact that a redistribution of the ion flux in the channel occurs, the number of particles recorded in the detector will change, depending on just what interstitial position the foreign is located in. Thus, as a result of the spatial redistribution of the ion flux in a crystal lattice, it turns out to be possible to determine the exact location of an impurity atom located in an interstitial position.

This fact has fundamental importance in a number of fields of solid-state physics, particularly in the physics of hyperfine interactions and solid-state radiation physics. We now turn to a detailed study of the question of redistribution of the flux of particles in the lattice.

b) Statistical equilibrium distribution in axial channeling. A statistical description of channeling was used by Lindhard.[18] This description is convenient for discussing the redistribution of a flux of particles.

The potential $U_t(r)$ created at a point r is the sum of the potentials of individual atomic strings, i.e.,

$$U_t(r)=\sum_{i=1}^{n} U(r-r_i), \tag{2.1}$$

where U is the potential of an individual string, r_i is the location of the string, and n is the number of atomic strings forming a channel. A particle hitting a crystal at a point r perpendicular to the transverse plane considered can have a transverse energy $E_\perp$ determined from the equation

$$E_\perp = U_t(r)=\frac{Mv_\perp^2}{2}; \tag{2.2}$$

$v_\perp$ is the transverse velocity, and M is the mass of the particle. This equality determines the region accessible to an ion with a given transverse energy.

At the beginning the beam of particles has some initial distribution in four-dimensional phase space. As it passes through the crystal, a tendency will be observed for establishment of statistical equilibrium. As a consequence of this, it is possible to go over to a statistical description of channeling, and not discuss in detail the series of collisions of ions with atomic strings.

As a result of the fact that in two-dimensional momentum space the volume is proportional to $dE_\perp$, it turns out that for particles with a given transverse energy $E_\perp$ the probability of location in an elementary area dS of the transverse plane, dW/dS, does not depend on r:

$$\frac{dW}{dS}=\begin{cases} 0, & E_\perp < U_t(r), \\ \dfrac{1}{S(E_\perp)}, & E_\perp > U_t(r), \end{cases} \tag{2.3}$$

where $S(E_\perp)$ is the region accessible for an ion with energy $E_\perp$. This formula shows that for axial channeling the ion uniformly fills the accessible region. This simple distribution occurs only in the two-dimensional case.[37]

c) Time of establishment of equilibrium distribution. The question of the possibility of using a statistical description, in particular Eq. (2.3), is discussed in the literature[27] up to the present time. It is therefore important to consider in sufficient detail the limits of applicability of the statistical approach.

It must be said first of all that if the system has stochastic irreversibility and intermixing properties, this system can be described statistically. Here it is particularly argued that because of the finite resolution of the physical apparatus we are always dealing with a small but finite volume in phase space.

Consider, for example, the yield of a nuclear reaction as a function of the depth when the particle beam is directed along the channel axis. As a result of the periodic nature of the particle motion in the channel, the yield also will oscillate with depth, but at large depths, because of the phase mixing of the particle trajectories, the oscillations will disappear.

At the same time, if we use Eq. (2.3) for calculation of this process, this description gives no oscillations.

The question therefore arises: at what depth can a statistical description be used?

Very small oscillations will exist up to extremely great depths. However, large-scale oscillations of the order of a quarter wavelength of the particle in the channel disappear rapidly as the result of the phase mixing. In this case the question of at what depths observation of oscillations is possible depends on the resolution of the detector. The characteristic resolution in depth of contemporary detectors amounts to a hundred angstroms. When a beam of protons and α particles with $E \sim 1$ MeV passes along a channel, in these detectors it is practically impossible to detect oscillation of yield after several oscillations of the ion in the channel. At the same time the average yield recorded by the detector at such small depths is predicted quite correctly when the calculation is carried out by means of Eq. (2.3).

It is clear that in a physical experiment where the dynamics of a system are followed for a finite time, we almost never have complete statistical equilibrium in a very small volume of phase space, but because of the finite resolution of the instrument there is no necessity of a probabilistic description of the evolution of this system in this case.

Lindhard,[18] using the potential $U(\rho)=\alpha_2/\rho$ (ρ is the distance from the string, $\alpha_2=(\pi/2)Z_1Z_2e^2a/d$), considered the question of scattering of an ion by atomic strings on the assumption that these strings are distributed at random. Here it turned out that an important change in the direction of the initial momentum of the ion occurs at depths of the order of λ, where

$$\overline{\lambda^{-1}} \approx \frac{\pi N\, d\alpha_2}{E_\perp} \tag{2.4}$$

for an ion with transverse energy $E_\perp$. For light ions with $E_\perp \approx E\psi_1^2$ ($E\psi_1^2$ is the critical transverse energy at which channeling is still possible) we have $\lambda < 1000$ atomic layers.

In channeling a particle moves at a distance greater

than a from the string, where it is best to use a potential of the type $U \sim \rho^{-2}$. For this potential[28] we have

$$\lambda^{-1} \approx \sqrt{3} N d a \psi_1, \qquad (2.5)$$

i.e., λ does not depend on the transverse energy; ψ_1 is the Lindhard critical angle.

The existence of a regular location of the strings has the result that for axial channeling the angular distribution may turn out to be asymmetric as a result of planar blocking.[28] Consequently, λ can approach 1 μ, which corresponds to experiment[29].

In spite of this effect of planes on axial channeling, the latter is substantially different from planar channeling. Special experiments[30] show that axial channeling is two-dimensional, due primarily to the potentials of the atomic strings, while planar channeling is one-dimensional.

The concept of accessibility of a region for axial channeling, used by Lindhard, is legitimate in spite of the existence of planes, as a result of the fact that the potential barriers and gradients of the atomic strings are substantially higher than those of planes.

Computer calculations[31] and experiments[32] confirm these basic ideas of Lindhard's theory.

In a number of cases the idea of an equilibrium distribution can be used if we have in mind only configuration space, i.e., the transverse plane in axial channeling. Actually, as the result of planar blocking, equilibrium in phase space sets in only at depths ~ 1 μ, but this does not mean that at smaller depths it is impossible to use an equilibrium distribution. In many cases it is not necessary to be interested in the onset of equilibrium in momentum space, i.e., in the angular distribution.

For example, in calculation of the flux of particles over the cross section of the channel, we are interested first of all simply in the total number of particles crossing the element of area considered, independent of the direction of these particles. The question naturally arises, at what depths can we use Eq. (2.3) in this case and how strongly does the asymmetry in the angular distribution affect the uniform filling of the accessible region?

In order to answer this question accurately, it is necessary to make a detailed calculation without use of Eq. (2.3) and a statistical calculation with Eq. (2.3), and to determine the depth at which the two calculations give an identical value with inclusion of the detector resolution.

Such calculations (see for example Sec. g of Chap. 2 and Sec. a of Chap. 3) show that for protons and α particles with $E \sim 1$ MeV the idea of equilibrium in configuration space can be used at depths of ~ 1000 Å. For heavier ions these depths are smaller.

While the angular distribution is still not symmetric (i.e., while there is still no equilibrium), as was noted above, planar blocking exists in axial channeling. This leads to the fact that in some places in the transverse plane a series of sites can be blocked, i.e., strictly speaking, Eq. (2.3) cannot be used here in the general case. Nevertheless there are a number of experiments where use of Eq. (2.3) has been justified even in this case. One of them is an experiment to determine the location of impurity atoms. Because of the symmetry of the crystal, any completely defined interstitial position in the transverse plane, as a rule, occupies not one but many sites. Therefore, even if some of these sites are blocked, we can speak of equilibrium in the transverse plane, since for the remaining sites the anisotropy in the angular distribution will have no effect in practice. Thus, in this case the asymmetry in the angular distribution will affect only weakly the uniform filling of the accessible region.

It is therefore clear that it makes sense to carry out special calculations in order to establish when we can use approximately the concept of uniform filling of the accessible region in the transverse plane.

The atomic strings produce in the transverse plane a potential close to harmonic. The trajectory of an ion in this field is an ellipse. Since the real potential contains also an anharmonic part, the ellipse is rotated and describes a figure of the Lissajous type which more or less uniformly fills the accessible region. In the course of two to three periods of oscillation of the ion in this field, rather uniform filling of the region is achieved. The depth at which this filling sets in is

$$\lambda \approx \frac{2\pi b^2}{a\sqrt{3}\, n \psi_1}, \qquad (2.6)$$

where n is the number of atomic strings forming a channel, b is the channel radius, ψ_1 is Lindhard's critical angle, and a is a screening parameter. Equilibrium sets in as the result of inelastic scattering of particles by electrons, and the anharmonicity of the potential facilitates a more rapid phase mixing of the particle trajectories. Equation (2.6) is valid for the greater part of the beam. For well channeled particles for which the anharmonic part of the potential is very small, equilibrium sets in at greater depths. However, the fraction of such particles in the beam is insignificant, as the result of scattering at the surface, beam divergence, and so forth. Kagan and Kononets[20] showed on a completely different basis that the distribution of channeled particles becomes independent of the initial conditions also at depths of the order of a thousand atomic layers.

d) Distribution of ion flux in an axial channel. Consider a unit flux of ions incident normally on the area S_0 associated with one axial channel. The area S_0 is not always equal to the area πr_0^2 which is associated with a single string. In the general case we can write $S_0 = \pi r_0^2 \alpha^{-1}$, where α is the ratio of the number of axial channels to the number of atomic strings forming the channel. In Si, for example, $\bar{\alpha} = 1/2$ in the ⟨110⟩ direction, $\bar{\alpha} = 1$ in the ⟨100⟩ direction, and $\bar{\alpha} = 2$ in the ⟨111⟩ direction.

In Fig. 1 we have shown the equipotential surfaces in

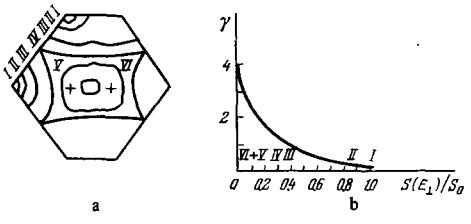

FIG. 1. Equipotential lines in Si in the ⟨100⟩ direction (a) and distribution of flux in the ⟨110⟩ channel in Si (b). The sign + shows tetrahedral interstitial positions.

Si and the effective flux. As can be seen from this figure, the maximum value of the flux in the center of the channel is greater than the flux at the periphery near the atomic string by about three orders of magnitude, i.e., the flux is substantially nonuniform.

The ion-redistribution effect can be explained as follows. The center of the channel is accessible to all ions, and ions with small transverse energies stay there for the most part. The peripheral part of the channel is accessible only to the small fraction of the ions with large transverse energy. This circumstance also explains the rapid change in the flux over the channel cross section.

We will estimate the ion flux F as some equipotential $\bar{S}(E_\perp)$ bounding a surface $S(E_\perp)$. If the transverse energy considered is not too small, its value is determined by the potential of one string, i.e., $E_\perp = U(\rho)$, where ρ is the distance from the string. Here $S(E_\perp) = \pi(r_0^2 - \rho^2)\bar{\alpha}^{-1}$. For normal incidence of the ions on the area S_0, the distribution of ions in minimum impact parameter ρ_1 relative to the chain has the form (for $\bar{\alpha} = 1$)

$$\frac{dn}{d\rho_1} = \frac{2\rho_1}{r_0^2}, \tag{2.7}$$

or

$$dn = \frac{dS}{S_0}. \tag{2.8}$$

The flux produced by ions having an accessible region from S to S + dS is $(1/S_0)dS/S$. The flux at some equipotential $\bar{S}(E_\perp)$ is produced only by those ions whose accessible region exceeds $S(E_\perp)$ and thus lies between $S(E_\perp)$ and S_0.

Hence we can see that the flux at the equipotential $\bar{S}(E_\perp)$ is

$$F = \frac{1}{S_0}\int_{S(E_\perp)}^{S_0}\frac{dS}{S} = \frac{1}{S_0}\ln\left|\frac{S_0}{S(E_\perp)}\right|. \tag{2.9}$$

If we take into account that a fraction of the ions equal to S_{un}/S_0 (where $S_{un}/S_0 = \pi r_{min}^2 Nd$) does not enter the channeling mode and that this fraction of the ions provides a normal contribution to the flux, the formula for the flux can be written more correctly:

$$F = \frac{1}{S_0}\left(\ln\left|\frac{S_0 - S_{un}}{S(E_\perp)}\right| + \frac{S_{un}}{S_0}\right). \tag{2.10}$$

Usually $S_{un}/S_0 \approx 10^{-2} \ll 1$, so that there is no practical difference between these two formulas.

The relative flux of ions in a channel, normalized to the flux for arbitrary unoriented irradiation, γ, is obviously

$$\gamma = \ln\left|\frac{S_0}{S(E_\perp)}\right|. \tag{2.11}$$

For small $E_\perp$, the value of $S(E_\perp)$ approaches zero, i.e., γ has a logarithmic singularity. For large $E_\perp$, the value of $S(E_\perp)$ approaches S_0 and in this case the flux at some small distance ρ from the string is

$$\gamma = \frac{\rho^2}{r_0^2}, \tag{2.12}$$

since for large $E_\perp$ we have $S(E_\perp) = \pi(r_0^2 - \rho^2)\bar{\alpha}^{-1}$. Comparing Eqs. (2.11) and (2.12), we see that in the limiting case of large $E_\perp$ we have $\gamma \ll 1$, while for small $E_\perp$ we have $\gamma \gg 1$, i.e., Eq. (2.10) describes also the blocking effect. These features of the ion flux redistribution in the transverse plane have the result that the cross section for scattering of ions by a defect (i.e., by an impurity or displaced atom) depends substantially on the location of the defect. Equations (2.9)—(2.12) are fundamental in the theory of the flux-redistribution effect. They were obtained previously in refs. 33—37.

e) Dependence of the flux on the angle of incidence of the ion beam on the crystal. In the preceding section we discussed the case in which the external angle $\psi_{in} = 0$. We will now consider the case in which $\psi_{in} \neq 0$. In order to carry out the analysis, we will first consider the change of potential in the channel with distance. In the central part of the channel the absolute value of the potential and the change of potential in some small length δr are small. At the same time near an atomic string the corresponding values are large, i.e., $(\delta U/\delta r)_{centr}\delta r \ll (\delta U/\delta r)_{per}\delta r$, where the subscripts respectively denote the central part of the channel and the peripheral part. When the ion hits the crystal at an angle ψ_{in} less than the critical angle for channeling, we can write

$$E_\perp = U(\rho) + E\psi_{in}^2 = U(\rho'), \tag{2.13}$$

where ρ is the point of incidence. When $\psi_{in} = 0$, the minimum impact parameter relative to the string is simply the point of incidence, i.e., ρ.

For $\psi_{in} \neq 0$, as the result of the additional transverse energy equal to $E\psi_{in}^2$, the ion can approach the string to a distance[1] ρ which is determined from Eq. (2.13). Here the accessible region obviously changes in comparison with that which existed for $\psi_{in} = 0$. However, if the ion hits the crystal in the peripheral region, i.e., near a string, the accessible region is practically unchanged, since there the value of the potential is large. Therefore the additional increase in transverse energy by an amount $E\psi_{in}^2$ is not greatly felt near the string. If the ion hits the crystal in the vicinity of the center of the channel, the accessible region increases sharply, so that the potential barrier there is very small. In the central part of the channel the potential can be taken as harmonic:

$$U_1(r) = \frac{n\alpha_1}{b^4}r^2, \tag{2.14}$$

where $\alpha_1 = Z_1Z_2e^2(Ca)^2/d$, $C \approx \sqrt{3}$, and b is the channel radius.

This potential is obtained by expansion in series of the potential of an individual atomic string $U = \alpha_1/\rho^2$ and summation over the n strings forming a channel.

If for $\psi_{in} = 0$ the ion hits the center of the channel, its accessible region is zero. If $\psi_{in} \neq 0$, then a region equal to $\pi E\psi_{in}^2/A$ is accessible, where $A = n\alpha_1/b^4$. For $\psi_{in} = 0$ the region in which the turning point for channeled ions is concentrated is $S_0 - S_{un}$. For an external angle $\psi_{in} \neq 0$, this region is approximately equal to $S_0 - S_{un} - \pi E\psi_{in}^2/A$.

Let us evaluate the relative flux at some equipotential line $\bar{S}_{l_0}$ bounding a surface S_{l_0} for $\psi_{in} \neq 0$. Let $S_{l_0} > \pi E\psi_{in}^2/A$. Evidently for $\psi_{in} = 0$ the fraction of ions which cannot reach the equipotential $\bar{S}_{l_0}$ is S_{l_0}/S_0, and for $\psi_{in} \neq 0$ this same fraction is $(S_{l_0} - \pi E\psi_{in}^2/A)/S_0$.

From this discussion we find, using the same method as in the preceding section, that

$$\gamma(\bar{S}_{l_0}) = \ln\left|\frac{S_0 - \pi E\psi_{in}^2 - S_{un}}{S_{l_0} - (\pi E\psi_{in}^2/A)}\right| + \frac{S_{un} + \pi E\psi_{in}^2/A}{S_0}. \tag{2.15}$$

For small initial angles ψ_{in} we have $(S_{un} + \pi E\psi_{in}^2/A)/S_0 \ll 1$, i.e.,

$$\gamma(\bar{S}_{l_0}) \approx \ln\left|\frac{S_0}{S_{l_0} - (\pi E\psi_{in}^2/A)}\right|. \quad (2.16)$$

For $\psi_{in} = 0$ we obtain the previous result. In the center of the channel where $S_{l_0} = 0$, we have

$$\gamma = \ln\left|\frac{S_0 A}{\pi E\psi_{in}^2}\right|. \quad (2.17)$$

An interesting feature of Eq. (2.16) is the presence of a logarithmic singularity for $\psi_{in}^2 = S_{l_0}A/\pi E$. The double and multiple peaks in the angular distribution of channeled ions are associated with these singularities (see Chap. 3 below).

The fact that in Eq. (2.16) the value of the flux has a maximum for $\psi_{in}^2 = S_{l_0}A/\pi E$ is explained simply. For angles $\psi_{in}^2 > S_{l_0}A/\pi E$ the ions have an accessible region $> S_{l_0}$, so that the value of $\gamma(S_{l_0})$ in this case is small. For $\psi_{in}^2 < S_{l_0}A/\pi E$ some fraction of the ions generally will not reach the equipotential $\bar{S}_{l_0}$. For $\psi_{in}^2 = S_{l_0}A/\pi E$ all ions reach $\bar{S}_{l_0}$, and the accessible regions lie in the interval $\{S_0, S_{l_0}\}$. Thus, for $\psi_{in}^2 \approx S_{l_0}A/\pi E$ the flux at a line $\bar{S}_{l_0}$ has a value close to the maximum value.

f) Multiple scattering and its effect on ion flux redistribution. In all of the equations given above it is assumed that the transverse energy of the ion $E_\perp$ remains constant. However, the transverse energy of the ion changes as the result of scattering by electrons, by thermal vibrations of lattice atoms, defects, and so forth.

As a consequence of the change of $E_\perp$, the accessible region $S(E_\perp)$ also changes, and this in turn changes the distribution of the flux in depth. Up to this time we have discussed the value of the flux in the channel immediately after establishment of statistical equilibrium of the distribution. Now let us trace the dependence of the flux on depth, for which it is necessary to calculate the multiple scattering.

The multiple scattering of channeled particles by electrons and nuclei decreases substantially in comparison with the scattering of particles in an unoriented target, since the trajectories of the channeled particles pass far from the nuclei in regions with low electron densities. Here multiple scattering has the nature of a fluctuation of the channeling angle. The solution of the problem of finding the angular distribution of the particles in the channel requires another approach, distinct from the usual approach in the theory of scattering in a uniform medium. This is due to the fact that multiple scattering is superimposed on the motion in the continuous potential of the nuclei. The problem of multiple scattering of channeled ions is of interest in itself. As a result of the fact that channeled ions do not pass close to the nuclei, the cross section for physical reactions (for example, nuclear reactions, production of radiation defects, nuclear bremsstrahlung, production of characteristic radiation, ionization, and so forth) changes substantially. However, if the ion is dechanneled, the cross section becomes normal. Therefore, for a broad class of problems associated with utilization of the channeling effect, it is necessary to know the dechanneling function.

Let us consider first the nonconservation of transverse energy as the result of ion scattering due to thermal vibrations of lattice atoms. The effect of thermal vibrations on channeling has also been discussed by Kadmenskiĭ et al.[122] Since the atoms are displaced from their equilibrium positions, a fluctuation force $\Delta \cdot F$ acts on the channeled particle, where $\overline{\Delta F^2} = \overline{(F - F')^2}$, where $F = -\nabla U(r)$, $F' = -\nabla U(r + \Delta r)$, and Δr is the displacement of the atom.

The increase of the transverse energy $\langle \delta E_\perp/\delta x \rangle$ per unit length is related to $\overline{\Delta F^2}$ by the expression

$$\frac{\langle \delta E_\perp \rangle}{\delta x} = \frac{d}{4E}\langle \overline{\Delta F^2} \rangle, \quad (2.18)$$

where the angle brackets denote averaging over the accessible region. Lindhard[18] calculated the value of $\overline{\Delta F^2}$ with an accuracy to terms of order $\sim \mu_\perp^2/r^2$, where $\mu_\perp^2$ is the mean square amplitude of thermal vibration. In many cases it is desirable to know a more accurate value of $\overline{\Delta F^2}$.

It has been shown[39,40] that with an accuracy $\sim u_\perp^4/r^4$ we have

$$\overline{\Delta F^2} = \frac{u_\perp^2}{2}\left[(F')^2 + \left(\frac{F}{r}\right)^2\right] + \frac{(u_\perp^2)^2}{4}\left[\frac{3}{4}\frac{F^2}{r^4} - \frac{1}{2}\frac{FF'}{r^3} - \frac{1}{4}\frac{(F')^2}{r^2} + \frac{1}{2}\frac{FF''}{r^2} + \frac{3}{2}\frac{F'F''}{r} + \frac{3}{4}(F'')^2 + F'F'''\right], \quad (2.19)$$

where

$$F = \frac{d}{dr}u(r), \quad F' = \frac{d}{dr}F, \quad F'' = \frac{d^2F}{dr^2} \text{ etc.} \quad (2.20)$$

The first term in Eq. (2.19) corresponds to Lindhard's expression. With use of Eq. (2.19) and a potential $U(r) = \alpha_2/r$ the increase in transverse energy is

$$\left\langle \frac{\delta E_\perp}{\delta x} \right\rangle = \frac{5}{16}\frac{u_\perp^2}{r_0^2}\frac{d}{E}\frac{E_\perp^4}{\alpha_2^4}\left(1 + 4\frac{u_\perp^2 E_\perp^2}{\alpha_2^2}\right). \quad (2.21)$$

The change $\delta E_\perp$ is due also to inelastic scattering by electrons. For simple estimates it is assumed that $\delta E_\perp$ is proportional to that part of the energy loss which is due to close collisions.[18]

Far from the nuclei, the increase $\delta E_\perp$ due to inelastic scattering by electrons is much greater than $\delta E_\perp$ due to thermal vibrations of the lattice atoms.

The increase $\delta E_\perp$ due to the discreteness of the atomic string is much less than the variation of $\delta E_\perp$ due to thermal vibrations,[41] and therefore this correction need not be taken into account. Recently Firsov[123] showed that the discreteness is negligible in channeling.

Lindhard[18] suggested that in many cases we can assume that the change in transverse energy with depth occurs smoothly, without fluctuations. This approximation of Lindhard's, which is known as the approximation of monotonic collection of transverse energy, has been used in a number of studies[42-46] for calculation of the dechanneling function. A systematic and rigorous solution of the problem has been given in refs. 47—49, where the diffusion of the particles in transverse energy space was taken into account. In refs. 47—50 an explicit form of the diffusion coefficient for channeling was obtained.

Since the increase in transverse energy $\delta E_\perp$ in Coulomb scattering described by the Rutherford formula is small in comparison with $E_\perp$, we can use the Fokker-Planck approximation to study the behavior of channeled ions. The Fokker-Planck equation for the distribution function $f(E, E_\perp, x)$ has the form (E is the total energy of the ion, and x is the depth)

$$\frac{\partial f}{\partial x} = -\frac{\partial}{\partial E_\perp}\left(\left\langle \frac{\Delta E_\perp}{\Delta x}\right\rangle f\right) + \frac{1}{2}\left(\left\langle \frac{\Delta E_\perp^2}{\Delta x}\right\rangle f\right) - \frac{\partial}{\partial E}\left(\left\langle \frac{\Delta E}{\Delta x}\right\rangle f\right), \quad (2.22)$$

where the averaging $\langle \ldots \rangle$ is carried out over the accessible region. The coefficients in Eq. (2.22) are related to each other by the expression

$$\frac{1}{2}\left\langle \frac{\Delta E_\perp^2}{\Delta x} \right\rangle = \left\langle \frac{\Delta E_\perp}{\Delta x} [E_\perp - U(r)] \right\rangle. \quad (2.23)$$

If we neglect the change in total energy, Eq. (2.22) can be rewritten in the form[47]

$$\frac{\partial f}{\partial x} = \frac{1}{S(E_\perp)} \left[\frac{\partial}{\partial E_\perp} S(E_\perp) D(E_\perp) \frac{\partial}{\partial E_\perp} \right] - \frac{\partial}{\partial E_\perp} \left[\left\langle \frac{\Delta E_\perp}{\Delta x} \right\rangle_{\text{brems}} S(E_\perp) f \right], \quad (2.24)$$

and the diffusion coefficient can be written in the two forms:

$$D = \frac{1}{2}\left\langle \frac{\Delta E_\perp^2}{\Delta x} \right\rangle = \frac{1}{S(E_\perp)} \int_0^{E_\perp} S(E'_\perp) \left\langle \frac{\Delta E_\perp}{\Delta x} \right\rangle dE'_\perp \quad (2.25)$$

or

$$D = \left\langle \frac{\Delta E_\perp}{\Delta x} (E_\perp - U(r)) \right\rangle. \quad (2.26)$$

These formulas provide the possibility of calculating analytically the diffusion coefficients in channeling.

For example, for a potential $U(r) = \alpha_2/r$ and for large transverse energies where $r_0^2 \gg r_1^2(E_\perp)$, where $E_\perp = U(r_1)$, we find that the diffusion coefficient due to scattering by electrons, D_e, is given by

$$D_e \approx \frac{Z_1^2 e^2 L_e}{4Er_0^2} E_\perp^2, \quad (2.27)$$

where $L_e = \ln|2mv^2/I|$, and I is the ionization potential of the atom. The corresponding diffusion coefficient due to scattering of channeled particles by thermal vibrations, D_{th}, is

$$D_{th} \approx \frac{u_\perp^2 dE_\perp^2}{16 r_0^2 \alpha_2^2 E} \left(1 + \frac{3u_\perp^2 E_\perp^2}{\alpha_2^2}\right). \quad (2.28)$$

From comparison of these two formulas it is evident that D_{th} increases with increase of $E_\perp$ much more rapidly than D_e (see Fig. 4 below).

At high energies where $E > (M/m)E_\perp^c$ (where $E_\perp^c$ is the critical transverse energy of Lindhard), we can neglect the last term in Eq. (2.24). If, further, we assume that $S(E_\perp) = \text{const}$, then the Fokker-Plack equation (2.24) goes over to the ordinary diffusion equation in transverse energy (the Fick equation). However, this pure diffusion approximation has the important deficiency that the redistribution of the flux of channeled particles cannot be described by this means.

It follows from Eqs. (2.22) and (2.24) that in the problem of departure of particles from a channel, in addition to the usual term taking into account the increase of the transverse energy, it is necessary to consider also the diffusion term.

At the same time, Eq. (2.24) is not the ordinary diffusion equation. In addition to the last term, a new feature here is the presence of the weighting function $1/S(E_\perp)$ in front of the square bracket and the factor $S(E_\perp)$ inside it.

The appearance of these factors is physically, in the last analysis, due to the fact that scattering of channeled ions occurs not in free space but in the field produced by the atoms of the crystal.

In derivation of the kinetic equation (2.24), the following assumptions are used:

1) The combined potential produced in the channel by the atoms of a string is replaced by the continuous potential of the atomic string.

2) Existence of statistical equilibrium is assumed.

3) The change in the ion energy as a result of inelastic scattering by electrons and thermal vibrations is assumed much less than the ion energy.

Assumption 1), as was shown by Lindhard[18], is completely acceptable. Assumption 2) leads to the result that Eq. (2.24) can be used only at depths ≥ 1000 Å. Assumption 3) is also completely justified, since in Coulomb collisions the main role is played by remote collisions for which the change in momentum or energy of the particle in one collision is negligible.

Equation (2.24) is the most general equation in the classical theory of channeling. All of the main features of passage of a channeled beam through a crystal are described on the basis of this equation.

Equation (2.24) describes not only channeling but also the blocking effect in which a particle is emitted from a crystal lattice site. Here it turns out that the last term in Eq. (2.24) which describes the change in transverse energy due to ionization loss exerts opposite effects on channeling and blocking. Inclusion of this term reduces the particle yield for channeling and increases it for blocking. This behavior of the particle yield, χ, is easily explained.

In channeling, the yield of backscattered particles is provided by particles which have increased their transverse energy to the critical value, and the energy loss acts to prevent increase of the transverse energy. In blocking, on the other hand, the yield of particles along the channel axis occurs as a result of the decrease in their transverse energy, and the energy loss assists this process. It turns out that even at small depths where the change in total energy ΔE is small so that $\Delta E/E \ll 1$, the yield in blocking, χ^{bl}, is substantially greater than the yield in channeling, χ^{ch}. Experiments[52,53] completely confirm this conclusion.

In order to compare the approximation of monotonic collection of transverse energy with the solution of the kinetic equation, a number of calculations have been carried out.[47-49] Figure 2 shows the dechanneling function obtained in the approximation of monotonic collection of transverse energy. Also shown is the result of calculations in the diffusion approximation.

As can be seen, for a rigorous solution of the kinetic equation, i.e., with account of diffusion in transverse momentum space, the fraction of dechanneled ions is found to be substantially less than in the approximation of monotonic collection of transverse energy. This is explained by the fact that with inclusion of the diffusion term we do not have a continuous departure of particles from the channel, but a spreading of the initial distribution function $f(E, E_\perp, x = 0)$ in transverse energy. This is clearly evident from Fig. 3, where we have shown the behavior of $F(E) = S(E_\perp)f(E, E_\perp, x)$ as a function of $E_\perp$ at various depths. As can be seen from this figure, at small depths the fraction of ions with small transverse energies is very high. With increasing depth a redistribution in $E_\perp$ occurs, the relative role of ions with small $E_\perp$ decreasing. It is evident that, although the peak of the function $S(E_\perp)f(E, E_\perp, x)$ is displaced downward, its location on the horizontal axis is not greatly changed

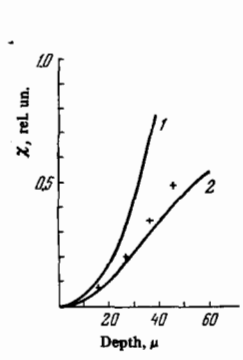

FIG. 2

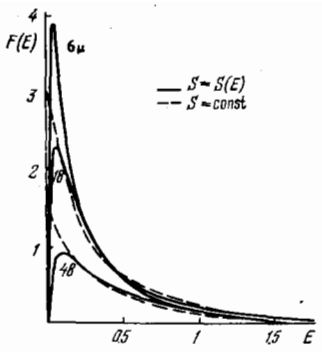

FIG. 3

FIG. 2. Dependence of fraction of dechanneled ions on depth in Si (⟨110⟩, t = 25°C). 1—approximation of monotonic accumulation; 2—diffusion approximation. The calculation was carried out for α particles with E = 7 MeV; the signs + show the experimental data of ref. 37.

FIG. 3 Variation of distribution function with depth in Si (⟨110⟩). The calculation was carried out for α particles with E = 7 MeV.

(i.e., in fact, a monotonic motion of this function to the right does not occur). At the same time, as the result of diffusion, a widening of the half-width of the function $f(E, E_\perp, x)$ takes place. For comparison we have shown in Fig. 3 a solution of Eq. (2.24) where $S(E_\perp)$ is assumed constant. As can be seen, the area under the curves are not greatly different, but the functional dependence in this case is not very accurate.

Determination of the dechanneling function is ordinarily carried out by means of experiments on backward scattering. Here it is customary to record particles which have left the channel near the surface, i.e., ions which in the channel have large transverse energies. These ions are dechanneled mainly as the result of scattering by thermal vibrations. This is evident from Fig. 4, where we have shown the dependence of the diffusion coefficient from electron and nuclear scattering on transverse energy. Here the diffusion coefficient due to electron scattering is not felt. Therefore in interpretation of these experiments the main dechanneling mechanism, electronic, has in essence been underestimated, and the nuclear mechanism due to thermal vibrations has been overestimated. The time spent by the main mass of ions in the channel is determined for normal incidence of the ion beam by electron scattering. In order to be sensitive to this, it is necessary to detect particles traveling at large depths. In Fig. 2 we have shown the results of such experiments.[41]

Solution of the kinetic equation (2.24) gives the possibility of solving the main problems associated with channeling of ions. For example, it is possible to obtain the dependence of the half-width of the dip in $\psi_{1/2}$ on temperature, depth, and so forth, and also a number of other important parameters.[48]

The main conclusion of this section is that the approximation of monotonic collection of transverse energy is unsatisfactory in many cases. It can be used only for rough estimates and then only near the surface when no more than 10–20% of the particles leave the channel. For a correct interpretation of the experiments it is necessary to use the solution of the kinetic equation with inclusion of the diffusion term.

The particle distribution function in transverse energy as a function of depth $f(E, E_\perp, x)$ permits calculation of the dependence of flux on depth. The flux is

$$\gamma(\mathbf{r}, x) = \int_{E_\perp^x}^{E_\perp^c} f[E, E_\perp, x]\, dE_\perp + \chi(x),$$

where $\chi(x)$ is the fraction of dechanneled ions, $E^x = U(r)$ is the potential energy of the ion in the channel at a given point r (r is the radius vector in the cross section of the channel), and $E^c = E\psi_1^2$.

Numerical calculations of the flux have been carried out for the case of passage of 3-MeV protons through silicon at room temperature in the ⟨110⟩ direction (Fig. 5).[48]

Since the equipotential line determined by the equation $E_\perp = U(r)$ gives a whole family of points at which the ion flux is identical, the dependence of the flux on the location r in the cross section of the channel was characterized by the reduced potential energy

$$\epsilon_\perp = \frac{2E_\perp^x}{E\psi_1^2}.$$

In Fig. 5 we have shown the dependence of the ion flux in the center of the channel and near an atomic string on the angle of incidence ψ_{in} at different depths. It can be seen from these data that the increase in flux is retained up to great depths ($\gtrsim 10\ \mu$), but initially it drops rapidly. At the same time an increase of flux with depth occurs at the atomic string. The dependence of the flux at various points of the channel on the angle of incidence at a depth 0.1 μ is given in Fig. 6. Note the existence of double peaks in the central part of the channel.

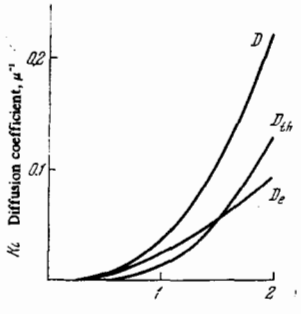

FIG. 4. Dependence of diffusion coefficients in transverse energy $\epsilon_\perp$ in Si (⟨110⟩, t = 25°C). D_e is the electronic diffusion coefficient, D_{th} is the nuclear diffusion coefficient ($D = D_e + D_{th}$).

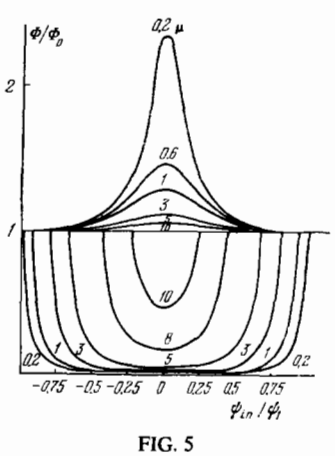

FIG. 5

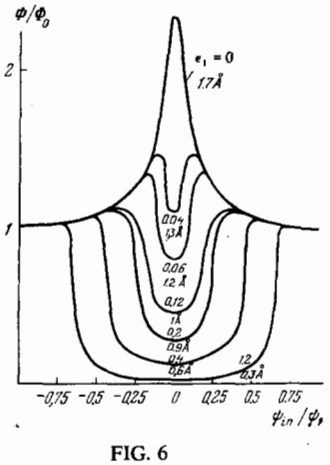

FIG. 6

FIG. 5. Dependence of flux in center of channel and near atomic string on angle of incidence ($\Phi/\Phi_0 = \gamma$). The calculation was carried out for protons with E = 3 MeV in Si (⟨110⟩, t = 25°C).

FIG. 6. Flux at different points of the ⟨110⟩ channel in Si at a depth 0.1 μ. The calculation was carried out for protons with E = 3 MeV (t = 25°C; the upper quantities are in units of $\epsilon_\perp$).

g) Distribution of ion flux at small depths. Up to this time we have discussed the flux at depths where an equilibrium distribution has been established. It is of interest to consider also small depths near the crystal surface.

The motion of the particles in the channel can be considered as the motion of Brownian particles in the field of the atomic strings. The scattering centers in the central part of the channel are the valence electrons, whose distribution in the channel can be considered isotropic.

The combined potential in a channel formed by n atomic strings has the form

$$U_t(r) = \frac{n\alpha_1 r^2}{b^4}\left(1 + \frac{r^2}{b^2}\right), \qquad (2.29)$$

if the potential of an individual string is given by the expression $u(\rho) = \alpha_1/\rho^2$, where $\alpha_1 = Z_1 Z_2 e^2 3a^2/d$, and b is the channel radius. In the central part of the channel we have $r/b < 1$, so that the anharmonic part of the potential is small there.

In the first approximation the motion of a particle can be considered in a two-dimensional harmonic well with axes y, z, where $y^2 + z^2 = r^2$.

For a Brownian particle in such a field it is possible to find a solution of the Fokker-Planck kinetic equation in phase space.

By means of this equation we can find the probability $W(y_0, z_0, y, z, \theta_{0y}, \theta_{0z}, x)$ that the particle will be at a point with coordinates (y, z) at a depth x if at $x = 0$ the particle enters the channel at an angle $\theta_0 = \sqrt{\theta_{0y}^2 + \theta_{0z}^2}$ at a distance $r_0 = \sqrt{y_0^2 + z_0^2}$ from the channel[54].

A formula for W can be obtained also by taking into account the anharmonicity of the potential. A feature of a harmonic potential is the fact that the flux calculated for such a potential changes periodically with depth. In spite of inelastic scattering by electrons, phase mixing of the trajectories occurs here only at very great depths. When the anharmonicity is taken into account, the tangling of the particle trajectories occurs much more rapidly.

In the anharmonic approximation the frequency of oscillations begins to depend on the point of entry of the particle into the channel. Here the "frequencies of oscillations" along the y and z axes have the following form:

$$\omega \approx \omega_0 \sqrt{\frac{M}{2E}}\left(1 + \frac{3}{4}\frac{y_0^2}{b^2}\right), \qquad \omega \approx \omega_0 \sqrt{\frac{M}{2E}}\left(1 + \frac{3}{4}\frac{z_0^2}{b^2}\right), \qquad (2.30)$$

where

$$\omega_0^2 = \frac{2n\alpha_1}{b^4 M}. \qquad (2.30)$$

The flux in an axial channel is

$$\gamma = \int\int W\, dy_0\, dz_0. \qquad (2.31)$$

In the harmonic approximation the flux can be calculated analytically:

$$\gamma = \frac{1}{4\cos^2\omega x}\left[\Phi\left(\frac{y\omega - \theta_{0y}\sin\omega x + \omega\bar{b}\cos\omega x}{\bar{\theta}^2}\right) - \Phi\left(\frac{y\omega - \theta_{0y}\sin\omega x - \omega\bar{b}\cos\omega x}{\bar{\theta}^2}\right)\right] \times \left[\Phi\left(\frac{z\omega - \theta_{0z}\sin\omega x + \omega\bar{b}\cos\omega x}{\bar{\theta}^2}\right) - \Phi\left(\frac{z\omega - \theta_{0z}\sin\omega x - \omega\bar{b}\cos\omega x}{\bar{\theta}^2}\right)\right] \qquad (2.32)$$

where Φ is the error integral, $\bar{b} = \frac{\sqrt{\pi}}{2}b$; $\bar{\theta}^2 = \frac{m}{2M}\frac{dE}{dx}\frac{x}{E}$, $\frac{dE}{dx}$ is the stopping power of the ion. As can be seen from this formula, the value of the flux oscillates with depth.

Figure 7a shows the dependence of the relative flux at the center of the channel on the depth, calculated by Van Vliet[58] by computer. It can be seen that the oscillations are damped at a depth ~2000 Å, which is in good agreement with the estimates made in section c) and also with calculations on the basis of Eq. (2.31).

At depths $\gtrsim$1000 Å for particles with E ~ 1 MeV the flux distribution given by Eq. (2.31) is essentially no different from the distribution in the transverse plane given by Eq. (2.3). Calculations of the yield of a nuclear reaction in the matrix atoms carried out by Ryabov[60] and Barret[61] give similar results.

Figure 7b shows a calculation carried out by means of Eq. (2.31) (curve 1). Curve 2 was calculated by solution of Eq. (2.24) on the assumption that statistical equilibrium exists. It is evident that, even without inclusion of the divergence of the beam due to inelastic scattering by electrons and anharmonicity, phase mixing sets in after traversal of about 1000 atomic layers.

In Figs. 8 and 9 we have shown the results of calculations of γ_{max} as a function of ion energy, orientation, ion-beam divergence, depth, and type of ion on the assumption that an equilibrium distribution exists.

In Fig. 8 we have given the energy dependence of the

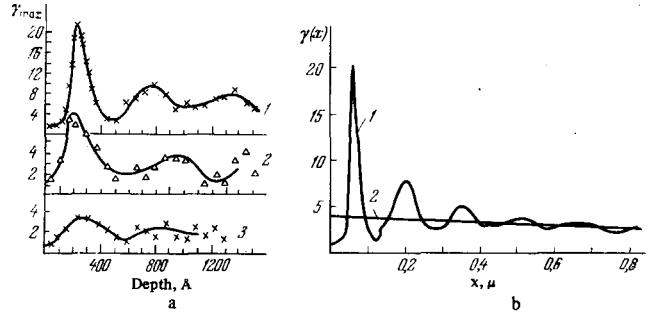

FIG. 7. a) Dependence of maximum flux of α particles with E = 1 MeV in Cu on depth (1—multiple scattering is not taken into account; 2—multiple scattering is taken into account (beam divergence $\theta = \pm 0.06°$); 3—the same as 2 but for $\theta = \pm 0.23°$ (calculation of Van Vliet by computer [58])); b) dependence of relative flux of protons in the center of the ⟨110⟩ channel in Si (E = 700 keV) on x (1—calculation with Eq. (2.31) with inclusion of anharmonicity in inelastic scattering by electrons; 2—calculation by solution of Eq. (2.24) on the assumption of existence of statistical equilibrium).

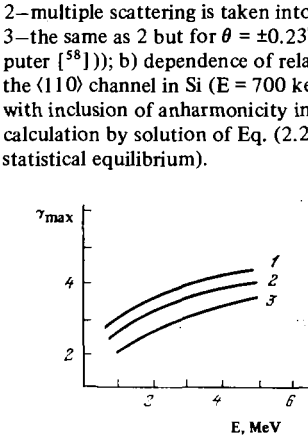

FIG. 8

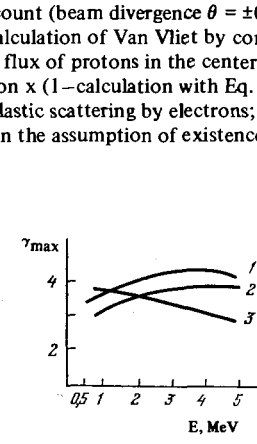

FIG. 9

FIG. 8. Dependence of maximum flux on energy and depth. α particles in Si (⟨110⟩, $\bar{\theta} = 0.01°$, $x(\mu) = 0.1$ (1), 0.2 (2), and 0.5 (3)).

FIG. 9. Energy dependence of maximum flux (Si, α particles). 1—electron scattering is considered to a depth of 0.1 μ ($\bar{\theta} = 0.02°$, ⟨110⟩); 2—the same for ⟨111⟩; 3—the same as 1 but for $\bar{\theta} = 0.1°$.

maximum flux at the center of the channel γ_{max}, with inclusion of multiple scattering by electrons. As can be seen, γ_{max} decreases with increasing depth. In the figure we have shown the case of small divergence ($\theta = 0.01°$). For a greater divergence γ_{max} will decrease with energy, i.e., there will be a pattern opposite to that which occurs in Fig. 9, where we have considered the case $\theta = 0.1°$.

In spite of the fact that the area S_0 associated with the ⟨110⟩ channel in Si is approximately five times the area of the ⟨111⟩ channel, γ_{max} in the two cases is rather similar, as can be seen from Fig. 8. This is simply explained by the fact that the coefficient A used to calculate the potential in the channel is proportional to U″(b). Therefore the small area is compensated, though incompletely, by the large change of U″(b) at small b, i.e., for channels with small S_0, since $S_0 \approx \pi b^2$.

In Figs. 10 and 11 we have shown the results of computer calculations by Alexander et al.[58,57] Detailed comparison of computer calculations at small depths with an analytical approach based on assumption of an equilibrium distribution is given in ref. 59. The good agreement of these two approaches is noted.

h) Splitting of the angular distribution of channeled ions and appearance of multiple peaks. When the foreign atom is localized at some equipotential line S_{l_0} bounding the area $\bar{S}_{l_0}$, according to Eq. (2.16) for $\psi_{in}^2 = S_{l_0}A/\pi E$ a logarithmic singularity occurs. Hence it is evident that in the angular distribution $\gamma(\psi_{in})$ the appearance of a double peak is possible.[38,62]

The appearance of the logarithmic singularity can be understood in the following way. For $\psi_{in} = 0$ for a part of the ions the equipotential $\bar{S}_{l_0}$ is inaccessible. For $\psi_{in}^2 = S_{l_0}A/\pi E$ this equipotential is accessible for all ions. If ψ_{in} exceeds this value, the accessible regions of the ions are increased, so that the flux at the line $\bar{S}_{l_0}$ in this case will be smaller than for $\psi_{in}^2 = S_{l_0}A/\pi E$. Thus, for $\psi_{in}^2 = S_{l_0}A/\pi E$ the flux at the line $\bar{S}_{l_0}$ will have a value close to the maximum.

Having determined the experimental value of ψ_{in} for which the peak appears, we can find the value of S_{l_0}, i.e., the location of the foreign atom. Thus, the angular distribution of channeled ions carries information on the location of impurity atoms. We will consider several cases of interest.[38,59]

If the impurity atom is localized in the center of the channel, the distribution is characterized by a maximum for $\psi_{in} = 0$ (Fig. 12a).

If the impurity atoms are localized in the central part of the channel at some equipotential $\bar{S}_l$, then a double peak appears (this is shown schematically in Fig. 12b).

If part of the impurity atoms are localized in the center of the channel and the other part in the central part of the channel, then a triple peak will appear.

If part of the impurity atoms are localized in the center of the channel and the other part is in substitutional positions, then there will be a maximum at $\psi_{in} = 0$, but the height of the maximum may not even reach the normal level (see Fig. 12c). The height of the peaks depends not only on the location of the impurity atom but also on what fraction of the impurity atoms occupy such a position.

If the impurity atoms are localized in the peripheral part of the channel, the maximum will be replaced by a minimum (Fig. 12d), but the half-width of this minimum will be smaller than the critical angle.

All of these features can be seen also in Fig. 6, where an accurate calculation has been made.

On taking into account the finite divergence of the beam, the logarithmic singularity in Eq. (2.16) disappears and the value of γ in this case is given by the formula[37]

$$\gamma = \ln \left| \frac{S_0}{S_{l_0} 2\psi_{in}(\theta)} \right|. \qquad (2.33)$$

Recently Alexander et al.[59,62] observed a multiple peak in Fe implanted with Br ions. The splitting of the angular distribution and the appearance of multiple peaks has an important significance, since it greatly facilitates the interpretation of experiments to determine the location of the impurity atom.

As was pointed out above, if the impurity atom is localized in the center of the channel, then for $\psi_{in} = 0$

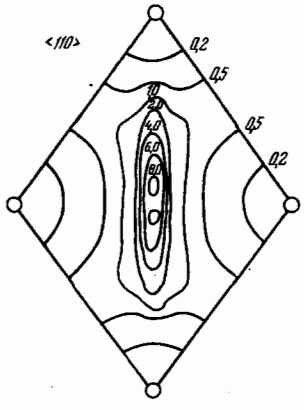

FIG. 10

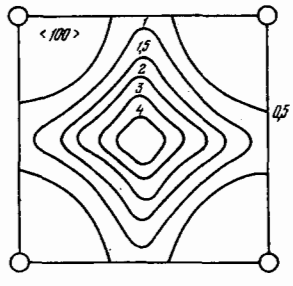

FIG. 11

FIG. 10. Contour plot of ⟨110⟩ channel in Cu with indication of flux values (computer calculation of Alexander et al. [56]) (in relative units).

FIG. 11. Contour plot of ⟨110⟩ channel of copper with indication of flux values [56] (in relative units).

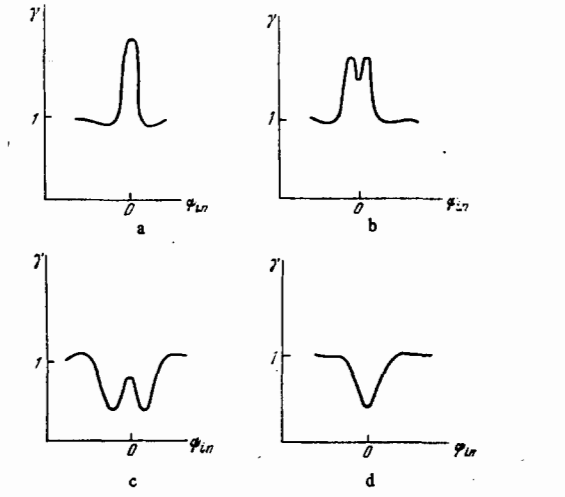

FIG. 12. Schematic representation of dependence of flux on initial angle of incidence of ion beam. a) Impurity atom in center of channel; b) impurity atoms in central part of channel but not exactly in center; c) part of impurity in center of channel, and remaining part in substitutional state; d) impurity atoms localized in peripheral part of channel near the atomic string.

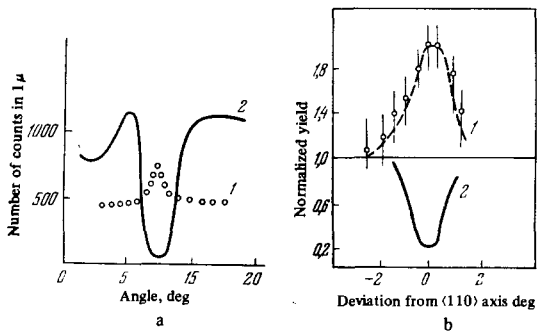

FIG. 13. Effect of yield increase in nuclear reactions. a) Increase of proton yield in the reaction $H^2(d, p)H^3$ (1) and yield of matrix atoms in niobium (2) (experiment of Iferov, Pokhil, and Tulinov [63a]); b) increase of yield of α particles in the reaction $Li^7(p, \alpha)He^4$ (1) and yield of matrix atoms in Si (2) (experiment of Andersen, Uggerhoj, and Gibson [63b]).

a peak appears in the angular distribution. An increase in yield has been observed experimentally in refs. 36, 56, and 63–68. In Fig. 13 we have shown an increase in the yield of nuclear reactions, which was observed for the first time in ref. 63.

A theoretical interpretation of the increased yield, based on the theory of ion flux redistribution, has been given by Kumakhov[33] (see also refs. 34, 35, 37) and also by Andersen et al.[36]. Computer calculations carried out at approximately the same time[55,56-59] also show the possibility of a yield increase. References 34–37 and 55–59 have pointed out the possibility of using the ion flux redistribution effect for accurate determination of the location of an impurity atom in an interstitial position. In principle it is possible also to obtain information on the amplitude of thermal vibration of the impurity atom.[33]

Alexander[56] has attempted to obtain information on the quantity $u_{\perp i}$—the amplitude of thermal vibration of an impurity atom located in a substitutional position, by measurement of the angular half-widths $\psi_{1/2}$ and $\psi_{1/2,i}$ in the matrix and impurity atoms.

3. EFFECT OF SPATIAL REDISTRIBUTION OF ION FLUX IN PLANAR CHANNELING

a) The flux of ions in a planar channel. Channeling occurs, as is well known[18], not only when the initial momentum of the particles is parallel to the principal crystallographic axes, but also in the case when the initial momentum is parallel to the principal atomic planes. This is so-called planar channeling. As in the case of axial channeling, we will avoid discussion of the particle motion along the planes, i.e., in depth, and discuss only motion in the plane perpendicular to the longitudinal momentum of the particle, i.e., we will consider one-dimensional motion between two planes.

The equilibrium distribution for one-dimensional motion (which we will designate as $\bar{f}(E_\perp, y)$) differs substantially from the two-dimensional case considered in section a of Chap. 2.

If we watch the motion of a particle for a time $t \gg T$ (T is the period of motion between the two planes), then

$$\bar{f}(E_\perp, y) = \begin{cases} \frac{2\,dt}{dy}\frac{1}{T(E_\perp)} = \frac{\sqrt{2M}}{T(E_\perp)\sqrt{E_\perp - Y(y)}}, & E_\perp > Y(y), \\ 0, & E_\perp < Y(y); \end{cases} \quad (3.1)$$

here $Y(y)$ is the potential of the plane, and y is measured from the plane. Note that the distribution (3.1) can also be obtained as a solution of the equation of continuity in phase space:

$$v_y \nabla_y \bar{f} + \frac{F}{M} \nabla_{v_y} \bar{f} = 0, \quad (3.2)$$

where $Mv_y^2/2 = E_\perp$. As can be seen from Eq. (3.1), in contrast to the two-dimensional case, a particle spends a large fraction of the time near the turning point, seeming to "hover" over the plane.

Suppose that a unit flux of ions enters one planar channel traveling in the parallel direction. Let us find the flux of ions at some distance z from the center between the two planes, when an equilibrium distribution (3.1) is established.

Obviously this flux is

$$\gamma(z) = \frac{2}{d_p}\int_z^l \bar{f}(E_\perp, z)\,dz_1, \quad (3.3)$$

where $Y(z_1) = E_\perp$, d_p is the distance between the atomic planes ($l = d_p/2$), and $z = l - y$.

In order to obtain a simple analytic formula for the flux, the potential in the planar channel can be assumed harmonic. In a detailed discussion it is necessary to take into account also the anharmonic term. If Molière's potential is used as the ion-atom potential, the potential $Y(z)$ with inclusion of both planes can be written in the form

$$Y(z) = \frac{V_0 b_1^2}{2}\left(z^2 + \frac{b_1^2 z^4}{12}\right), \quad (3.4)$$

where

$$V_0 = 0.3\xi\,\frac{8\pi N z_1 z_2 e^2 l}{b_1}\exp\left(-\frac{b_1 l}{l}\right), \quad b_1 = \frac{0.3}{a}.$$

In the approximation which takes into account only the harmonic part of the potential (3.4),

$$\bar{f}(E_\perp, z) = \begin{cases} \frac{\sqrt{V_0 b_1^2/2}}{\pi\sqrt{E_\perp - (V_0 b_1^2/2)z^2}}, & E_\perp > \frac{V_0 b_1^2}{2} z^2, \\ 0, & E_\perp < \frac{V_0 b_1^2}{2} z^2. \end{cases} \quad (3.5)$$

Then the flux in the channel, $\gamma(z)$, is equal to

$$\gamma(z) = \frac{2}{\pi}\ln\left|\frac{l}{z} + \sqrt{\left(\frac{l}{z}\right)^2 - 1}\right|. \quad (3.6)$$

Hence it is evident that in the central part of the channel for $l/z \gg 1$, we have $\gamma > 1$, i.e., the flux in the center of the channel is higher than the normal flux.

The flux distribution in the channel described by Eq. (3.6) is illustrated in Fig. 14. As can be seen from this figure, in the peripheral part of the channel near the atomic plane, the relative flux is substantially less than unity.

The case of an inclined beam, where peaks in the angular distributions can arise, and also the effect of beam divergence on the value of the flux, has been discussed in an earlier article.[37]

The estimates made above are valid only for those depths for which $t \gg T$, i.e., where the particle com-

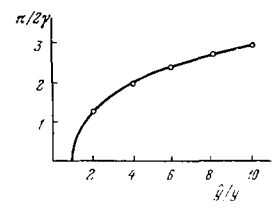

FIG. 14. Distribution of ion flux in planar channel.

pletes at least several oscillations between the two planes. In investigation of the near-surface layers it is desirable to calculate the flux more accurately without use of the equilibrium distribution (3.1). This necessity arises, for example, in the case where the detector energy resolution permits analysis of very thin near-surface layers of the crystal.

As in Sec. g of Chap. 2, for solution of this problem we can use the analogy between a Brownian particle and a channeled ion, assuming that the distribution of valence electrons in which the ion scattering occurs is uniform.

On the basis of a solution of the Fokker-Planck kinetic equation, we can find the probability $W(z_0, z, \theta_0, x)$ that the ion will be at a point with coordinate z at depth x if for x = 0 the ion enters the channel at an angle θ_0 at a distance z_0 from the center of the channel. This probability is expressed by the formula[54]

$$W(z_0, z, \theta_0, x) = \frac{\omega}{\sqrt{\pi\bar{\theta}^2}} \exp\left[-\frac{1}{\bar{\theta}^2}(z\omega - z_0\omega\cos\omega x - \theta_0 \sin\omega x)^2\right]. \tag{3.7}$$

When a harmonic potential is used, we have $\omega = \omega_0\sqrt{\frac{M}{2E}}$, $\omega_0^2 = \frac{v_0 b_1^2}{M}$; $\bar{\theta}^2$ is the mean square angle of scattering by electrons after traversing a depth x: $\bar{\theta}^2 \approx \frac{m}{2M}\frac{dE}{dx}\frac{x}{E}$; $\frac{dE}{dx}$ is the stopping power of the ion.

On taking into account the anharmonicity, ω begins to depend on the initial coordinate z_0:

$$\omega \approx \omega_0\sqrt{\frac{M}{2E}}\left(1 + \frac{3}{8}\frac{b_1^2}{6}z_0^2\right). \tag{3.8}$$

The relative flux $\gamma(z, x)$ as a function of depth is obviously given by the formula

$$\gamma(x, z) = \int_{-l}^{l} W\, dz_0. \tag{3.9}$$

For a harmonic potential in this case we obtain the simple formula

$$\gamma = \frac{1}{2\cos\omega x}\left[\Phi\left(\frac{z\omega - \theta_0\sin\omega x + l\omega\cos\omega x}{\bar{\theta}^2}\right) - \Phi\left(\frac{z\omega - \theta_0\sin\omega x - l\omega\cos\omega x}{\bar{\theta}^2}\right)\right]. \tag{3.10}$$

It can be seen from this that the flux oscillates with depth. The maximum flux in the center of the channel (i.e., for z = 0), when the beam is incident on the crystal in a direction parallel to the plane considered, has the value

$$\gamma_{max}(x) = \frac{1}{\cos\omega x}\Phi\left(\frac{l\omega\cos\omega x}{\bar{\theta}^2}\right). \tag{3.11}$$

Using the simple formulas (3.9)–(3.11), we can interpret experiments near the surface.

b) Multiple scattering of channeled ions in planar channeling. An important difference exists between axial and planar channeling, in view of the fact that in motion along a plane at a large angle to the crystallographic axes, in contrast to the axial case, successive collisions occur with very different impact parameters. Therefore nuclear scattering, in addition to a directing effect, and contrary to the case of axial channeling, exerts an important effect on the diffusion of the particles in their transverse energy, even if thermal vibrations are omitted from the discussion.

An equation of the Fokker-Planck type for planar channeling has been obtained in earlier articles.[48,69] If we neglect the change in total energy, the equation has the form

$$\frac{\partial F}{\partial x} = \frac{1}{2}\frac{\partial}{\partial E_\perp}\left[\left\langle\frac{\Delta E_\perp^2}{\Delta x}\right\rangle T\frac{\partial}{\partial E_\perp}\left(\frac{F}{T}\right)\right], \tag{3.12}$$

where x is the depth, $E_\perp$ is the transverse energy, and T is the period of motion of the particle in the channel. In many applications it is convenient to use the following relation:

$$T\left\langle\frac{\Delta E_\perp}{\Delta x}\right\rangle = \frac{1}{2}\frac{\partial}{\partial E_\perp}\left(T\left\langle\frac{\Delta E_\perp^2}{\Delta x}\right\rangle\right). \tag{3.13}$$

In Eq. (3.4)–(3.5) the angle brackets designate averaging over the period of oscillation of the particle:

$$\langle X\rangle = \frac{4}{T}\int\frac{X\, dy}{\sqrt{(E_\perp - Y)\,2/M}}, \tag{3.14}$$

where Y is the planar potential. In a number of cases a solution of Eq. (3.12) can be obtained in explicit form.[48] In Table I we have given the calculated depths $x_{1/2}$ at which the number of particles in the channel is decreased by a factor of two. These values were obtained as the result of solution of Eq. (3.12).

As can be seen, there is good agreement between the theory and the experiments of Davies et al.[70]. Hence we can conclude that the calculation of $x_{1/2}$ can serve as a good estimate for theoretical prediction of this quantity in design of an experiment.

4. CHANNELING OF HEAVY IONS

a) Some features of heavy-ion channeling. As was pointed out in section f) of chapter 2, for $(M/m)\psi_1^2 > 1$ the decrease in transverse energy due to energy loss exceeds the increase due to scattering by electrons. The condition $(M/m)\psi_1^2 > 1$ is satisfied at not very high velocities for heavy particles. For example, in Si in channeling of protons this condition is satisfied already at energies of the order 0.1 MeV and below. With decrease of the transverse energy the accessible region $S(E_\perp)$ decreases. This leads to the result that with increasing depth there is an increase in the flux in the center of the channel, rather than a decrease as for fast light particles. In Fig. 15 we have shown a calculation of the flux for deuterons with E = 300 keV, carried out by computer[66,67]. As can be seen, with increasing depth the flux increases. It is evident that near the surface, where a statistical equilibrium distribution

TABLE I. Depth $x_{1/2}(\mu)$ at which half of a channeled beam of protons in tungsten leaves the channel

Direction (plane)	Energy, MeV	$x_{1/2}, \mu$ theory	$x_{1/2}, \mu$ experiment [70]
{100}	2	1.5	1.3
	3	2.2	2.8
	6	4.4	4.0
{111}	2	2.6	2.7
	3	3.9	4.1
	6	7.8	8.8

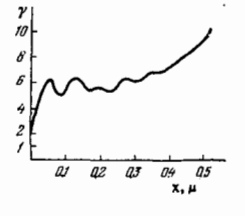

FIG. 15. Dependence of flux on depth for deuterons with E = 300 keV in niobium. [66,67]

has not yet been established, the flux oscillates with depth.

Some fraction of the ions with large transverse energies are dechanneled as a result of scattering by lattice nuclei undergoing thermal vibrations. In this way the channeled beam is split into two components[48]. Ions with small $E_\perp$ as a result of energy loss to electrons are focused toward the channel axis, while ions with large $E_\perp$ leave the channel. On the average the ranges of the two kinds of ions can differ considerably. This leads to a very substantial difference between the profile of implanted ions under conditions of channeling and the profile in an amorphous medium.

The problem of the spatial distribution of implanted ions in crystals has acquired considerable interest recently as a result of the extensive use of the technique of ion implantation of conductors. A great many articles have been devoted to this question[71-98]. The features of heavy-ion channeling appear distinctly in discussion of the question of the spatial distribution of these ions. This question is briefly discussed below.

b) Spatial distribution of heavy channeled ions. In calculation of the profile of implanted ions in an amorphous medium (i.e., without taking into account channeling) it is sufficient to know the projected range and the straggling. In a crystal, when channeling is taken into account, the situation is substantially more complicated. As we will see, the profile depends on a very large number of parameters. For simplification of the calculations a number of assumptions will be made:

1) If the ion has a transverse energy below Lindhard's critical energy, the ion is considered channeled.

2) If the ion has an energy above the critical value, it is assumed that the ion belongs to the random part of the beam.

3) Capture of an ion back into a channel is not taken into account.

4) The crystal is assumed to be ideal—i.e., scattering of ions on the defects introduced during the implantation is neglected.

5) It is assumed that the transverse energy increases monotonically, i.e., diffusion in transverse momentum space is not taken into account.

The change in transverse energy $\epsilon_\perp$ at the velocities considered $v \leq v_0 = 2.2 \times 10^8$ cm/sec is due mainly to energy lost to electrons $(\Delta\epsilon_\perp/\Delta x)_e$ and scattering $(\Delta\epsilon_\perp/\Delta x)_S$, and also to scattering by thermal vibrations, $(\Delta\epsilon_\perp/\Delta x)_{th}$, i.e.,

$$\left\langle\frac{\Delta\varepsilon_\perp}{\Delta x}\right\rangle=\left\langle\frac{\Delta\varepsilon_\perp}{\Delta x}\right\rangle_e+\left\langle\frac{\Delta\varepsilon_\perp}{\Delta x}\right\rangle_{th}+\left\langle\frac{\Delta\varepsilon_\perp}{\Delta x}\right\rangle_S; \tag{4.1}$$

here the angle brackets designate averaging over the accessible region. Usually the last term in Eq. (4.1) is substantially smaller than the first two terms. For fast light particles, as is well known, the last term is dominant. Equation (4.1) has been solved in two approximations.[48] In the first case, which we will call the rectangular well approximation, it is assumed that the average kinetic transverse energy is equal to the total transverse energy, i.e.,

$$\left\langle\frac{\Delta\varepsilon_\perp}{\Delta x}\right\rangle_e=\frac{\varepsilon_\perp}{E}\left\langle\frac{\Delta E}{\Delta x}\right\rangle, \tag{4.2}$$

where $\langle\Delta E/\Delta x\rangle$ is the change in total energy. In the second approximation, where the potential in the channel is assumed harmonic, in accordance with the virial theorem we have

$$\left\langle\frac{\Delta\varepsilon_\perp}{\Delta x}\right\rangle=\frac{1}{2}\frac{\varepsilon_\perp}{E}\left\langle\frac{\Delta E}{\Delta x}\right\rangle. \tag{4.3}$$

Lindhard's formulas[18] are used for the quantities $\langle\Delta\epsilon_\perp/\Delta x\rangle_{th}$ and $\langle\Delta\epsilon_\perp/\Delta x\rangle_S$. In this case

$$\left\langle\frac{\Delta\varepsilon_\perp}{\Delta x}\right\rangle_S=\frac{d\sqrt{5mv^2\hbar\omega_p}}{4EZ_1Z_2e^2}\left\langle\frac{\Delta E}{\Delta x}\right\rangle. \tag{4.4}$$

In the rectangular well approximation for the potential, Eq. (4.1) can be rewritten in the form

$$\left\langle\frac{d\varepsilon_\perp}{dE}\right\rangle=\frac{\varepsilon_\perp}{E}+\left\langle\frac{d\varepsilon_\perp}{dx}\right\rangle_{th}\left\langle\frac{dE\,(E_\perp)^{-1}}{dx}\right\rangle+\frac{d\sqrt{5mv^2\hbar\omega_p}}{4EZ_1Z_2e^2}. \tag{4.5}$$

In the harmonic approximation the first term on the right-hand side in Eq. (4.5) is replaced by $\epsilon_\perp/2E$. Equation (4.5) is solved by computer by a method similar to that used in ref. 48. The method provides the possibility of investigating the effect of the main factors on which the channeled-ion profile depends: to study the effect of the amorphous layer which usually covers the surface of a crystal, the dependence on orientation and on temperature, and the dependence of the profile on the initial angle of incidence of the ion beam, energy, and so forth.

In Fig. 16 we have shown the energy dependence of the profile for boron ions channeled along the ⟨111⟩ direction in Si at room temperature. As can be seen, with increasing angle the fraction of ions falling into the channel for a given thickness Δx of the amorphous layer covering the surface increases. In addition, the depth of both the first and second maxima increases.

In Fig. 17 we have shown the energy dependence for phosphorous ions.

In Fig. 18 we have shown the orientation dependence of the profile for boron ions with E = 50 keV.

As can be seen, in the ⟨110⟩ direction the range of the channeled ions is substantially greater than in the ⟨111⟩ direction. This is also confirmed by experiments.[74]

There is a great difference in the profiles for ions of B and P if all conditions are equal. This is explained by the fact that the range of boron ions in the amorphous medium and in the channel do not differ so

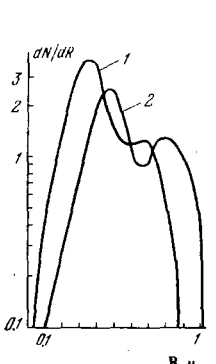

FIG. 16

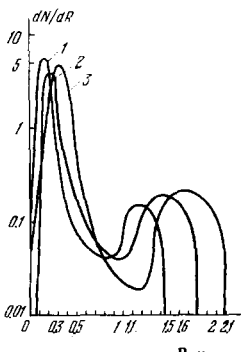

FIG. 17

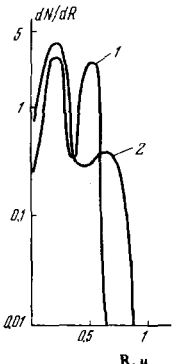

FIG. 18

FIG. 16. Energy dependence of profile for boron ions in the ⟨111⟩ direction in Si. 1–E = 100 keV, 2–E = 150 keV. The thickness of the amorphous layer is $\Delta x = 50$Å.

FIG. 17. Dependence of profile for P ions on energy in Si (⟨110⟩, t = 25°C). E_0(keV) = 100 (1), 150 (2), and 200 (3). $\Delta x = 50$Å.

FIG. 18. Dependence of profile for boron ions with E = 50 keV in silicon on orientation (1–⟨111⟩, $\Delta x = 20$Å; 2–⟨110⟩, $\Delta x = 100$Å).

greatly as in the case of phosphorus. Therefore the first and second maxima for boron ions are more difficult to separate experimentally than in the case of phosphorus ions.

This circumstance is aggravated also by the fact that scattering by thermal vibrations is weaker for boron ions than for phosphorus ions. Therefore the depth of the dip between the first and second maxima for boron ions is substantially smaller than for phosphorus ions. The heavier the ion, the more distinctly should the dip between the first and second maxima appear. In Fig. 19 we have shown the experimental profile for P ions obtained by Dearnaley and co-workers.[71] As can be seen, there are two clearly expressed maxima. The maximum ranges of the channeled ions can be calculated with the theoretical estimates for the energy loss as a function of impact parameter.[96-97]

5. EXPERIMENTS TO DETERMINE THE LOCATION OF IMPURITY ATOMS

a) The main factors affecting the location of an impurity atom. When impurity atoms are introduced in the lattice by means of diffusion, they usually replace atoms of the matrix. In ion implantation, which we are discussing here, the location varies, Ion implantation is a substantially nonequilibrium process. In implantation, radiation damage (Frenkel pairs), disordered regions, and so forth, are produced. As a consequence of this, in implantation, impurity atoms can occupy various locations in the lattice. We will consider a number of factors which can affect the location of an impurity atom introduced into the crystal by means of implantation.

In the process of stopping of an ion in a crystal, a rather large number of displaced atoms and vacancies are produced along the track. The ion can interact with a vacancy and can occupy a substitutional position.

The impurity atom can become substitutional also on annealing of disordered regions.

Impurity atoms can also occupy an interstitial position. In silicon, for example, one of these positions is the tetrahedral interstitial position. There are several channels by which the transition of an impurity atom to an interstitial position can take place. For example, this can occur in the direct interaction of a matrix atom with an impurity atom located in a substitutional state.[26] As a result the matrix atom occupies its site, and the impurity atom occupies an interstitial position. In addition, there can be simply a transition of the impurity atom to the tetrahedral interstitial position, as a result of which there occurs vacancy formation and filling of the tetrahedral interstitial position. This reaction has been observed experimentally for ions of thallium implanted in silicon.[26]

Impurity atoms can also occupy other locations. Dislocations and other imperfections can serve as a natural sink for impurity atoms. They can emerge also onto the surface of a crystal.

A detailed analysis of experiments carried out up to 1970 is contained in the book by Mayer, Eriksson, and Davies.[26] The quantitative, and in a number of cases even the qualitative interpretation of these experiments are not satisfactory, since in these studies the effect of ion flux redistribution was not taken into account. Nevertheless, it is possible to indicate several factors and basic regularities which have been observed experimentally. The radiation dose and temperature at which the implantation is carried out substantially affect the location of the impurity atom. There is also a dependence on the annealing temperature.

A definite correlation exists of the fraction of ions located in substitutional states with the number of radiation defects and the temperature.[26]

In Table II we have enumerated the main experiments carried out up to 1970 in silicon.[99-116]

The behavior of the impurity atom in the lattice also depends on its charge state. Therefore the elements of different groups of the periodic table behave differently. Elements of group IV and V for the most part occupy in silicon a substitutional position[26], while group II elements occupy generally an interstitial tetrahedral position. We will discuss in detail a number of new experiments in whose interpretation the redistribution of the channeled-particle flux has been taken into account.

b) Use of the flux redistribution effect for accurate determination of impurity atom location. In the work of Domeij, Fladda, and Johansson[65] the location of Zr, Hf, Tl, and Hg ions has been determined in silicon. The measurements were made with a beam of carbon ions of energy 1.8 MeV. These authors observed an increase in the yield in the ⟨110⟩ direction when the yield of silicon ions was measured (Fig. 20). At the same time in bombardment along the ⟨111⟩ direction the usual

TABLE II. Experiments to determine location of impurity atoms in silicon

Implanted ion	Experimental method	References
Li	(p, α)-reaction	99
B	(p, α)-reaction	100–103
P	β-emission	99
Ga	Backscattering	104, 105, 106–108
As	The same	100, 106–107
Cd	» »	109, 106
In	» »	100, 106, 110
Sn	» »	106
Sb	» »	100, 104, 106, 107, 111
Sb	X-ray emission	112
Tl	Backscattering	109, 106
Xe	The same	110
Cs	» »	106
Tm	» »	113
Yb	β-emission	114
Tl	Backscattering	100, 110, 115
Bi	The same	106, 116

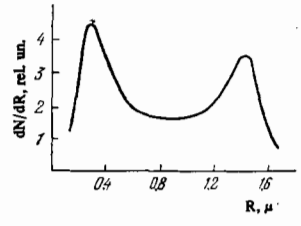

FIG. 19. Profile of P ions in Si, obtained experimentally. [71]

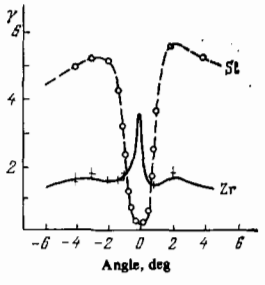

FIG. 20. Dependence of yield of Si matrix atoms and Zr impurity atoms on external angle (experiment of Domeij, Fladda, and Johansson [65]).

minimum was observed. This permitted the authors[65] to prove that the zirconium ions were localized in tetrahedral interstitial sites. In fact, for bombardment along the ⟨111⟩ direction the tetrahedral interstices are blocked by the ⟨111⟩ atomic string. At the same time along the ⟨110⟩ direction they lie in the central part of the channel (see Fig. 1a) and the yield γ is close to 2.3 (Fig. 1b). In ref. 65 the yield turned out to be 2.2.

In the variation of the yield of thallium ions (Tl) a minimum with a small peak in the center was observed along the ⟨110⟩ axis (Fig. 21). The yield along the ⟨111⟩ direction was insignificant. This gave the authors[65] the possibility of proving that a fraction of the Tl atoms occupy a tetrahedral site and the remaining fraction are in a substitutional state. According to the theoretical model (see Fig. 12) for the situation which was observed for thallium in ref. 65, part of the atoms are in a substitutional state and part are localized in an interstitial site. Since a minimum is observed along the ⟨111⟩ direction, the interstice for thallium ions corresponds to a tetrahedral position. Furthermore, since the yield for thallium ions is close to 1 along the ⟨110⟩ direction (if all thallium ions were localized in tetrahedral interstices, the yield γ according to Fig. 1b should be close to two), we can estimate that the fraction of ions located in a tetrahedral site is close to 1/2, and the remaining half are in a substitutional state.

In the work of Carstanjen and Sizmann[67] the location of deuterium atoms in niobium was determined by means of the nuclear reaction D(d, p)T. The target temperature was 150°K and the initial beam energy was 300 keV. From general thermodynamic considerations it is known that in the niobium lattice there can be tetrahedral, octahedral, and hexagonal interstitial positions. A theoretical calculation of the ion flux was carried out for all of these positions. Results of the calculations are shown in Fig. 22 by the solid lines. Then the identical experiment was performed. As can be seen Fig. 22, the result of the experiment agrees with the theory only in the case where the deuterium is in the tetrahedral interstitial positions. From this fact the authors[67] concluded that deuterium atoms in niobium are located in tetrahedral interstitial positions. It is interesting to note that this result is confirmed by the experiment of Somenkov et al.[117] on the basis of neutron diffraction. In the case of the experiment of Carstanjen and Sizmann[67] it is evident how important the theory of the flux redistribution is for interpretation of experiments to determine impurity atom location.

Andersen et al.[36] determined the location of ytterbium atoms implanted in silicon. A beam of 1-MeV α particles was used. Figure 23 shows the result of the experiment along the three principal axes. To explain the experiment the authors[36] considered two possibilities: 1) part of the Yb atoms (30%) were localized in tetrahedral interstitial positions, and the remaining part of the atoms were displaced rather far from the ⟨110⟩ and ⟨111⟩ axes and therefore do not provide a substantial decrease in the yield, 2) all Yb atoms are localized in one interstitial site which does not correspond to the ordinary tetrahedral interstitial position. If the Yb atoms were localized in tetrahedral interstitial positions, they should give a very low yield along the ⟨111⟩ and ⟨100⟩ directions, since along these rows this position is blocked. From this fact Andersen et al.[36] reached the conclusion that a third of the atoms lie along equivalent axes ⟨$\bar{1}$00⟩, and the remaining

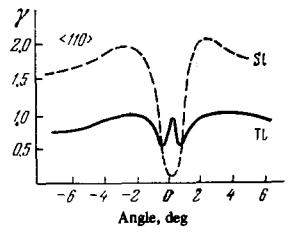

FIG. 21. Yield for thallium ions. [65]

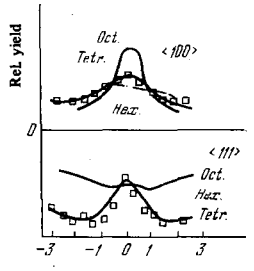

FIG. 22. Result of the experiment of Carstanjen and Sizmann. [66] The solid curves are the result of calculation of the flux by computer.

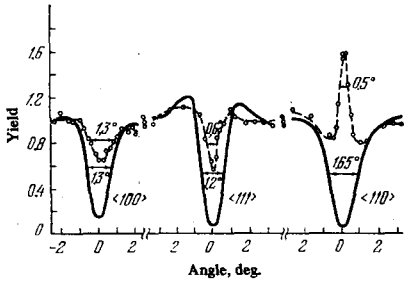

FIG. 23. Result of the experiment of Andersen et al. [36] on determination of the location of Yb in Si. The yield is in relative units.

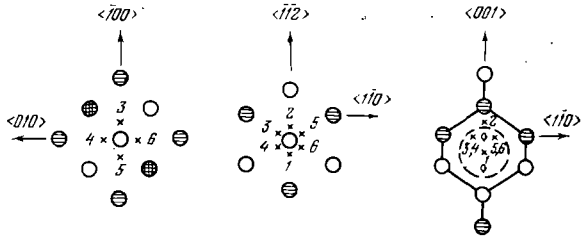

FIG. 24. Location of Yb atoms in Si along principal axial channels in Si.

atoms are displaced 0.68 Å from these axes (Fig. 24).

In Fig. 24 we have shown the locations of Yb atoms along the principal axes. As can be seen, along the ⟨1$\bar{1}$0⟩ axis 5/6 of the Yb atoms lie in the central part of the channel. Therefore along this axis an increase of yield is observed.

In the work of Eisen and Uggerhoj[68] the experiment of Andersen et al.[36] was repeated. In Fig. 25 we have shown the result of Eisen and Uggerhoj.[68] In contrast to the work of Andersen et al.,[36] the latter experiment[66] gave a yield of Yb atoms with a half-width not equal to the half-width of the yield of Si atoms, i.e., the matrix atoms. Therefore Eisen and Uggerhoj[68] made the assumption that Yb atoms in a number of cases can occupy two different interstitial positions. The difference of their results from those of ref. 36 is explained by Eisen and Uggerhoj, in particular, by the fact that the conditions of implantation of Yb atoms in silicon were somewhat different in the two experiments, and this can naturally lead to different results, as is clear from Sec. a of Chap. 5.

An experiment by Alexander, Callaghan, and Poate (see refs. 59, 62) determined the location of bromine atoms implanted in iron. This is one of the most accurate and complicated experiments carried out up to the present time. The authors observed for the first time a triple peak along the {211} plane (Fig. 26).

A detailed analysis of the experiment showed that 40% of the atoms are in a substitutional state, and the remaining 60% occupy an interstitial position. Here it turned out that these positions do not correspond to the ordinary tetrahedral interstitial positions. The authors reached the conclusion that for correct interpretation of the experiment it is necessary to carry out an analysis of the angular distribution along several principal crystallographic axes and planes. This experiment has demonstrated that the appearance of fine structure, i.e., multiple peaks, in the angular distributions greatly facilitates the interpretation of the experiments. In spite of the fact that implanted bromine atoms were placed not far from the surface (~400 Å), computer calculations and an analytical approach based on the assumption of establishment of an equilibrium distribution gave approximately identical results.

In the work of Matyash, Skakun, and Dikiĭ[119] the flux-redistribution effect has recently been used to determine the location of implanted atoms of oxygen in niobium. These authors experimentally obtained multiple peaks in axial and planar channels. This enabled them to show that oxygen impurity atoms occupy octahedral interstitial sites inside the unit cell.

c) Determination of the location of boron in silicon.

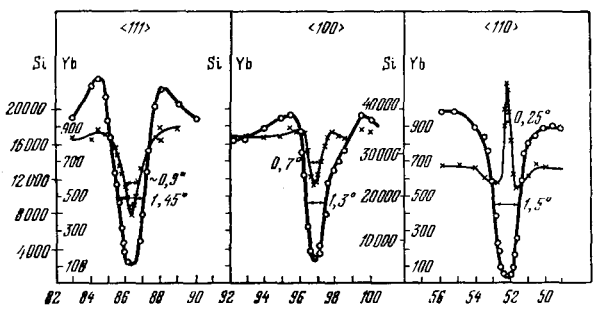

FIG. 25. Result of the experiment of Eisen and Uggerhoj [68] on determination of the location of Yb in Si.

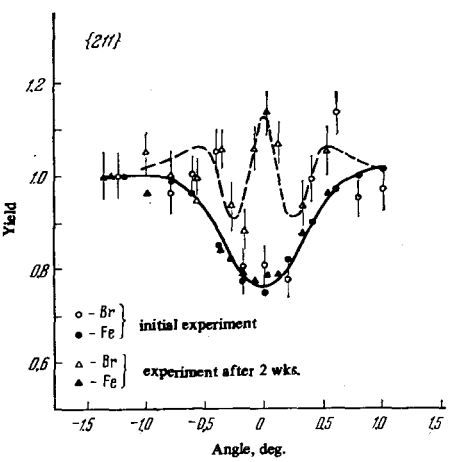

FIG. 26. Triple peak in Fe in which Br ions have been implanted (experiment of Alexander, Callaghan, and Poate [59,62,118]).

The theory of the flux-redistribution effect has recently been used[120] to determine the location of implanted atoms of boron in the silicon lattice.

The implantation was carried out with boron ions of energy 50 keV (dose 6×10^{14} cm^{-2}). The nuclear reaction B(p, α)Be was utilized, and the proton energy was E = 700 keV.

Figure 27 shows the results of measurements along the principal axial channels. These data were obtained after annealing at a temperature of 500°C. The experimental data indicate the presence of central peaks in scanning across the ⟨100⟩ and ⟨111⟩ axes, and double peaks in scanning across the ⟨110⟩ axis.

The results were compared with a calculation of the normalized yield as a function of the angle of incidence of the beam. The yield was found by calculation of the relative flux of protons in the respective channels.

By solution of a kinetic equation of the Fokker-Planck type, the change in transverse energy due to scattering by electrons, thermal vibrations, and defects was taken into account. The calculations and their comparison with experiment show that about 20% of the boron atoms are in substitutional states, and the remaining 80% in interstitial positions.

The best agreement of theory and experiment (Fig. 27) is achieved in the case when it is assumed that the boron atoms lie along the ⟨110⟩ axis at a distance of 0.97 Å from the substitutional position. The position found is shown in Fig. 28. As can be seen, it does not agree with the tetrahedral or hexagonal interstitial positions. On annealing, when $t \geq 500$°C, a quadruple peak is observed along the ⟨110⟩ direction. This can be explained by the fact that in this case boron occupies positions along the ⟨111⟩ diagonal, halfway between the closest atoms.

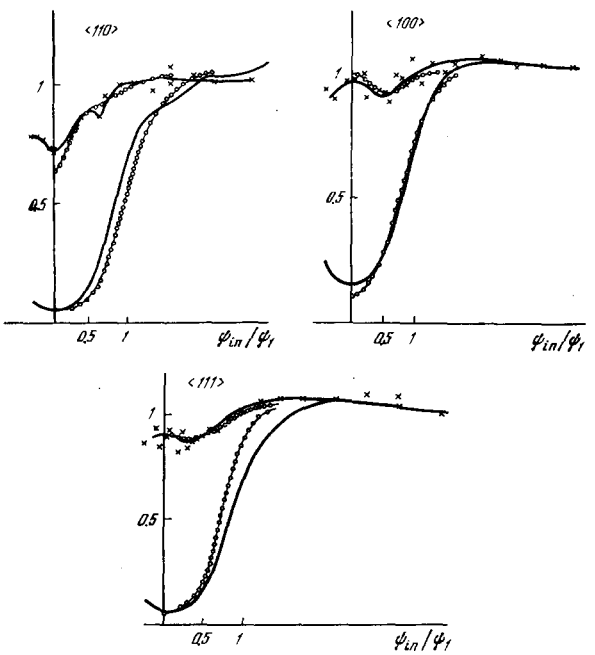

FIG. 27. Result of experiment on determination of the location of B in Si. The crosses designate the experimental yield, and the circles are theoretical (the solid curves are the yield of matrix atoms, and the circles are the theory).

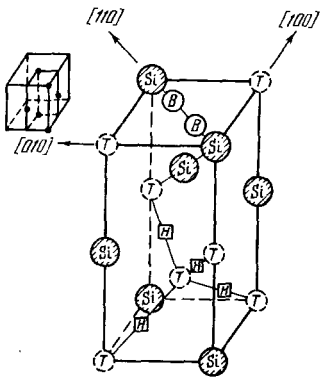

FIG. 28. Unit cell of silicon. T and H are the tetrahedral and hexagonal interstitial sites, and B is the location found for the boron atom. [120]

6. CONCLUSION

Up to the present time many studies have been made in which the channeling technique and the flux-redistribution effect have been utilized to determine the location of implanted atoms.

We have not discussed here studies in which the orientation effects have been used to determine the profile of implanted atoms and radiation defects, to determine the number of residual defects, to study the dynamics of annealing of defects, and so forth.

In contrast to optical and electrical measurements, the present method gives correct information on the exact location of the implanted impurity.

In crystals with a high density of defects, the channeling technique with use of the flux-redistribution theory has a number of important advantages over EPR, Mössbauer, and other techniques.

Use of characteristic x rays for identification of atomic sites in a lattice will subsequently provide, apparently, the possibility of obtaining necessary information even in those cases where the concentration of the implanted impurity is many orders of magnitude less than the concentration of the matrix atoms.

In conclusion I wish to express my deep gratitude to O. B. Firsov for his constant interest in my work and for numerous helpful discussions. I am grateful to B. B. Kadomtsev, Yu. V. Martynenko, A. A. Rukhadze, and B. M. Smirnov for their interest in this work and for helpful remarks.

[1] M. M. Bredov, R. F. Komarova, and A. R. Regel', Dokl. Akad. Nauk SSSR 99, 69 (1954); 113, 795 (1957).
[2] J. A. Davies, J. Friesen, and J. D. McIntyre, Can. J. Chem. 38, 1526 (1960).
[3] G. K. Wehner, J. Appl. Phys. 26, 1056 (1955).
[4] R. H. Silsbee, J. Appl. Phys. 28, 1246 (1957).
[5] P. K. Rol, J. M. Fluid, E. P. Vienböck, and M. de Jong, in Proc. of 4th Intern. Conf. on Ionization Phenomena in Gases, Amsterdam, p. 257, 1960.
[6] V. A. Molchanov and V. G. Tel'kovskiĭ, Dokl. Akad. Nauk SSSR 136, 801 (1961) [Sov. Phys. Doklady 6, 137 (1961)].
[7] E. S. Mashkova, V. A. Molchanov, and D. D. Odintsov, Dokl. Akad. Nauk SSSR 151, 1074 (1963) [Sov. Phys. Doklady 8, 806 (1964)]; Fiz. Tverd. Tela 5, 3426 (1963) [Sov. Phys. Solid State 5, 2516 (1964)].
[8] D. D. Odintsov, Fiz. Tverd. Tela 5, 1114 (1963) [Sov. Phys. Solid State 5, 813 (1963)].
[9] Yu. V. Martynenko, Fiz. Tverd. Tela 6, 2003 (1964) [Sov. Phys. Solid State 6, 1581 (1965)].
[10] M. T. Robinson and O. S. Oen, Phys. Rev. 132, 2385 (1963).
[11] R. S. Nelson and M. W. Thompson, Phil. Mag. 8, 1677 (1963).
[12] G. R. Piercy, F. Brown, J. A. Davies, and M. McCargo, Phys. Rev. Lett. 10, 399 (1963).
[13] G. Dearnaley, IEEE Trans. Nucl. Sci. NS-11, 249 (1964).
[14] B. Domeij and K. B. Björkqvist, Phys. Lett. 14, 127 (1965).
[15] A. F. Tulinov, V. S. Kulikauskas, and M. M. Malov, Phys. Lett. 18, 304 (1965); Dokl. Akad. Nauk SSSR 162, 546 (1965) [Sov. Phys. Doklady 10, 463 (1965)].
[16] D. S. Gemmell and R. E. Holland, Phys. Rev. Lett. 14, 945 (1965).
[17] V. M. Agranovich, S. A. Kurkin, and D. D. Odintsov, Preprint, Physics and Power Engineering Institute, No. 53, 1966.
[18] J. Lindhard, K. Dan. Vidensk. Selsk. Mat.-Fys. Medd. 34, No. 14 (1965).
[19] J. Lindhard, Phys. Lett. 12, 126 (1964).
[20] Yu. Kagan and Yu. V. Kononets, Zh. Eksp. Teor. Fiz. 58, 226 (1970); 64, 1042 (1973); 66, 1693 (1974) [Sov. Phys.-JETP 31, 124 (1970); 37, 530 (1973); 39, 832 (1974)].
[21] P. Lervig, J. Lindhard, and V. Nielsen, Nucl. Phys. A96, 481 (1967).
[22] N. P. Kalashnikov, M. I. Ryazanov, and F. I. Chukhovskiĭ, Zh. Eksp. Teor. Fiz. 54, 822 (1968); 63, 1107 (1972) [Sov. Phys. JETP 27, 441 (1968); 36, 583 (1972)].
[23] C. S. Newton and L. T. Chadderton, Radiat, Eff. 10, 33 (1971).
[24] Atomic Collisions and Penetration Studies, Proc. of the Intern. Conf., Can. J. Phys. 46, 6 (1968).
[25] Atomic Collision Phenomena in Solids, ed. D. W. Palmer, M. W. Thompson, and P. D. Townsend, Amsterdam, North-Holland, 1970.
[26] J. W. Mayer, L. Eriksson, and J. A. Davies, Ion Implantation in Semiconductors (Academic, New York, 1970). Russ. transl. Mir, Moscow, 1973.
[27] J. H. Barrett, Phys. Rev. Lett. 31, 1542 (1973).
[28] V. V. Beloshitskiĭ and M. A. Kumakhov, Fiz. Tverd Tela 15, 1588 (1973) [Sov. Phys. Solid State 15, 1060 (1973)].
[29] D. D. Armstrong, W. M. Gibson, et al., Radiat. Eff. 12, 143 (1972); A. A. Bednyakov, Yu. N. Zhukova, G. A. Iferov, V. S. Kulikauskas, A. F. Tulinov, and V. L. Chernov, in Trudy V. Vsesoyuznogo soveshchaniya po fizike vzaimodeĭstviya zaryazhennykh chastits s monokristallami (Proceedings of the Fifth All-Union Conference on the Physics of Interaction of Charged Particles with Single Crystals), Moscow, Moscow State University, 1974, p. 178.
[30] E. Bøgh, Radiat. Eff. 12, 13 (1972).
[31] G. Della Mea, A. V. Drigo, S. L. Russo, and P. Mazzoldi, et al., Phys. Rev. B7, 4029 (1973).
[32] M. J. Pedersen, J. U. Andersen, D. J. Elliot, and E. Laegsgaard, in Abstracts of Intern. Conf. on Atomic Collisions in Solids, Gatlinburg, 1973, p. 32.
[33] M. A. Kumakhov, Preprint, Moscow State University, L-p22178, Moscow, 1970, part II.
[34] M. A. Kumakhov, Phys. Lett. A32, 538 (1970).
[35] M. A. Kumakhov, Dokl. Akad. Nauk SSSR 196, 1300 (1971); 203, 794 (1972) [Sov. Phys. Doklady 16, 109 (1972); 17, 348 (1972)].
[36] J. U. Andersen et al., Radiat. Eff. 7, 25 (1971).
[37] M. A. Kumakhov, Radiat. Eff. 15, 85 (1972).

[38] M. A. Kumakhov, Phys. Lett. A39, 191 (1972).
[39] H. E. Schiøtt, E. Bonderup, and J. U. Andersen, cited in ref. 32, p. 31.
[40] M. A. Kumakhov, cited in ref. 32, p. 30.
[41] V. V. Beloshitsky, Yu. V. Bulgakov, and M. A. Kumakhov, Phys. Lett. A40, 181 (1972).
[42] G. Foti, F. Grasso, R. Quattrocchi, and E. Rimini, Phys. Rev. B3, 2169 (1971).
[43] K. Morita and N. Itoh, J. Phys. Soc. Japan 30, 1430 (1971).
[44] K. Björkqvist, B. Cartling, and B. Domeij, Radiat. Eff. 12, 267 (1972).
[45] R. Behrisch, B. M. U. Scherzer, and H. Schulze, Radiat. Eff. 13, 33 (1972).
[46] S. U. Campisano et al., Phys. Lett. A35, 119 (1971); G. Foti et al., Nuovo Cimento Lett. 4, 707 (1970).
[47] V. V. Beloshitskiĭ and M. A. Kumakhov, Zh. Eksp. Teor. Fiz. 62, 1144 (1972) [Sov. Phys. JETP 35, 605 (1972)].
[48] V. V. Beloshitsky, M. A. Kumakhov, and V. A. Muraler, Radiat. Eff. 13, 9 (1972); 20, 95 (1973).
[49] E. Bonderup, H. Esbensen, U. Andersen, and H. E. Schiøtt, Radiat. Eff. 12, 261 (1972).
[50] M. Kitagawa and Y. H. Ohtsukhi, Phys. Rev. B8, 3117 (1973).
[51] V. V. Beloshitskiĭ and M. A. Kumakhov, Zh. Eksp. Teor. Fiz. 66, 1783 (1974) [Sov. Phys. JETP 39, 876 (1974)].
[52] S. U. Campisano, G. Foti, F. Grasso, and E. Rimini, cited in ref. 2, p. 26.
[53] V. S. Andreev, V. N. Bogaev, N. K. Golubkov, A. A. Puzonov, and A. F. Tulinov, in Trudy III Vsesoyuznogo soveshchaniya po fizike vzaimodeĭstviya zaryazhennykh chastits s monokristallami (Proceedings of the Third All-Union Conf. on Physics of Interaction of Charged Particles with Single Crystals), Moscow, Moscow State University, 1972, p. 140.
[54] M. A. Kumakhov, in Tezisy VI Vsesoyuznogo soveshchaniya po fizike vzaimodeĭstviya zaryazhennykh chastits s monokristallami (Proceedings of the Sixth All-Union Conf. on Physics of Interaction of Charged Particles with Single Crystals), Moscow, Moscow State University, 1974, p. 13.
[55] R. B. Alexander, G. Dearnaley, D. V. Morgan, and J. M. Poate, Phys. Lett. A32, 365 (1970).
[56] R. B. Alexander, Ph. D. Thesis (Oxford University, 1971).
[57] R. B. Alexander, G. Dearnaley, D. V. Morgan, J. M. Poate, and D. Van Vliet, in Proc. of European Conf. on Ion Implantation, Reading, England, 1971, p. 181.
[58] D. Van Vliet, Radiat. Eff. 10, 137 (1971).
[59] R. B. Alexander, P. T. Callaghan, and J. M. Poate, Preprint (1973); Phys. Rev. B9, 3022 (1974).
[60] V. A. Ryabov, Zh. Eksp. Teor. Fiz. 63, 1096 (1972) [Sov. Phys. JETP 36, 577 (1973)].
[61] J. H. Barret, Phys. Rev. B3, 1527 (1971).
[62] R. B. Alexander and P. T. Callaghan, Phys. Lett. A45, 379 (1973).
[63] a) G. A. Iferov, G. P. Pokhil, and A. F. Tulinov, ZhETF Pis. Red. 5, 250 (1967) [JETP Lett. 5, 201 (1967)]; J. U. Andersen, E. Uggerhoj, and W. M. Gibson, in Proc. of the Conf. on Application of Ion Beams to Semiconductor Technology, Grenoble, France, 1967, p. 153.
[64] F. W. Saris, D. Onderlinden, and W. F. Van der Weg, cited in ref. 25, p. 540.
[65] B. Domeij, G. Fladda, and N. G. E. Johansson, Radiat. Eff. 6, 155 (1970).
[66] N. D. Carstanjen and R. Sizmann, Radiat. Eff. 12, 225 (1972).
[67] N. D. Carstanjen and R. Sizmann, Phys. Lett. A40, 93 (1972).
[68] F. Eisen and E. Uggerhoj, Radiat. Eff. 12, 233 (1972).
[69] V. V. Beloshitskiĭ and M. A. Kumakhov, Dokl. Akad. Nauk SSSR 212, 846 (1973) [Sov. Phys. Doklady 18, 652 (1974)].
[70] J. A. Davies et al., Phys. Rev. 165, 345 (1968).
[71] P. P. Goode, M. A. Wilkins, and G. Dearnaley, Radiat. Eff. 6, 237 (1970).
[72] R. A. Moline, J. Appl. Phys. 42, 3553 (1971).
[73] E. Bøgh, Radiat. Eff. 7, 115 (1971).
[74] F. Eisen, Can. J. Phys. 46, 587 (1968).
[75] E. I. Zorin et al., Fiz. Tverd. Tela 6, 3222 (1964) [Sov. Phys. Solid State 6, 2577 (1965)].
[76] V. M. Gusev et al., Fiz. Tverd. Tela 8, 1708 (1966) [Sov. Phys. Solid State 8, 1363 (1966)].
[77] I. B. Amirkhanova, I. G. Gverdtsiteli, A. I. Kuldamashvili, et al., in Radiatsionnaya fizika nemetallicheskikh kristallov (Radiation Physics of Nonmetallic Crystals), vol. III, Kiev, Naukova dumka, 1971, p. 111.
[78] R. I. Garber, A. K. Gnap, V. S. Krykhtin, and A. I. Fedorenko, in Radiatsionnaya fizika nemetallicheskikh kristallov (Radiation Physics of Nonmetallic Crystals), vol. III, Kiev, Naukova Dumka, 1971, p. 122.
[79] R. I. Garber, I. G. Gverdtsiteli, A. K. Gnap, A. I. Guldamashvili, A. A. Modlin, and A. I. Fedorenko, in Radiatsionnaya fizika nemetallicheskikh kristallov (Radiation Physics on Nonmetallic Crystals), vol. III, Kiev, Naukova Dumka, 1971, p. 133.
[80] M. A. Kumakhov, cited in ref. 33, preprint, parts III and IV.
[81] V. A. Eltekov, D. S. Karpusov, Yu. V. Martinenko, and V. E. Yurasova, in Proc. of the Intern. Conf. on Atomic Collisions, Brighton, 1970, p. 657.
[82] Yu. V. Martynenko, Fiz. Tverd. Tela 13, 2580 (1971) [Sov. Phys. Solid State 13, 2166 (1971)].
[83] M. A. Kumakhov and V. A. Muralev, Fiz. Tekh. Poluprovdn. 6, 1564 (1972) [Sov. Phys. Semicond. 6, 1350 (1972)].
[84] A. Desalvo, R. Rosa, and F. Zignani, Nuovo Cimento Lett. 2, 390 (1971).
[85] N. A. Ukhin, Fiz. Tekh. Poluprovdn. 6, 931 (1972) [Sov. Phys. Semicond. 6, 804 (1972)].
[86] E. Bøgh, Can. J. Phys. 46, 653 (1968).
[87] N. S. Romanov and L. S. Smirnov, Fiz. Tekh. Poluprovdn. 6, 1631 (1972) [Sov. Phys. Semicond. 6, 1410 (1972)].
[88] E. I. Zorin, P. V. Pavlov, D. N. Tetel'baum, and A. F. Khokhlov, Fiz. Tekh. Poluprovdn. 7, 2006 (1973) [Sov. Phys. Semicond. 7, 1340 (1973)].
[89] V. M. Gusev, M. I. Guseva, E. S. Ionova, A. N. Mansurova, and V. K. Starinin, Fiz. Tekh. Poluprovdn. 7, 2153 (1973) [Sov. Phys. Semicond. 7, 1435 (1973)].
[90] F. Eisen and B. Welch, Radiat. Eff. 7, 143 (1971).
[91] Fizicheskie osnovy ionno-luchevogo legirovaniya (Physical Basis of Ion Implantation), A collection edited by P. V. Pavlov, Gor'kiĭ, Gor'kiĭ State University, 1972.
[92] V. S. Vavilov, N. U. Isaev, B. N. Mukashev, and A. V. Spitsyn, Fiz. Tekh. Poluprovdn. 6, 1041 (1972) [Sov. Phys. Semicond. 6, 907 (1972)].
[93] V. M. Kolyada, V. G. Zlobin, and I. A. Zaporozhets, Fiz. Tekh. Poluprovdn. 6, 1813 (1972) [Sov. Phys. Semicond. 6, 1565 (1972)].

[94]G. A. Gumanskiĭ and I. S. Tashlykov, Inzh.-Fiz. Zh. 21, 1105 (1971).
[95]V. S. Vavilov, M. A. Gukasyan, E. A. Konorova, and Yu. V. Milyutin, Fiz. Tekh. Poluprovdn. 6, 2384 (1972) [Sov. Phys. Semicond. 6, 1998 (1972)].
[96]F. F. Komarov and M. A. Kumakhov, Phys. Stat. Sol. 58, 389 (1973).
[97]B. E. Baklitsky and E. S. Parilis, Radiat. Eff. 12, 137 (1972).
[98]I. G. Gverdsuteli, A. I. Guldamashvili, E. M. Diasamidze, S. A. Zaslavskii, A. N. Kalinin, M. A. Kumakhov, and V. A. Muralev, Radiat. Eff. 19, 171 (1973).
[99]W. M. Gibson, F. W. Martin, R. Stensgaard, F. Palmgren-Hensen, N. I. Meyer, G. Galster, A. Johansen, and J. S. Olsen, Can. J. Phys. 46, 675 (1968).
[100]J. A. Davies, J. Denhartog, L. Eriksson, and J. W. Mayer, Can. J. Phys. 45, 4053 (1967).
[101]G. Fladda, K. Björkqvist, L. Eriksson, and D. Sigurd, Appl. Phys. Lett. 16, 313 (1970).
[102]L. Eriksson, J. A. Davies, J. Denhartog, H. Matzke, and J. L. Whitton, Can. J. Phys. 5, 40 (1966).
[103]J. C. North and W. M. Gibson, Appl. Phys. Lett. 16, 126 (1970).
[104]J. W. Mayer, L. Eriksson, S. T. Picraux, and J. A. Davies, Can. J. Phys. 46, 663 (1968).
[105]J. W. Mayer, J. A. Davies, and L. Eriksson, Appl. Phys. Lett. 11, 365 (1967).
[106]L. Eriksson, J. A. Davies, N. G. E. Johansson, and J. W. Mayer, J. Appl. Phys. 40, 842 (1969).
[107]L. Eriksson, G. Fladda, and K. Björkqvist, Appl. Phys. Lett. 14, 195 (1969).
[108]L. Eriksson, J. A. Davies, and J. W. Mayer, in Radiation Effects in Semiconductors, ed. F. Vook, N. Y. Plenum Press, 1968, p. 398.
[109]S. T. Picraux, N. G. E. Johansson, and J. W. Mayer, in Semiconducting Silicon, ed. R. Haberecht and E. Kern, N. Y., Electrochem. Soc., 1969, p. 422.
[110]J. A. Davies, L. Eriksson, and J. W. Mayer, Appl. Phys. Lett. 12, 255 (1968).
[111]L. Eriksson, J. A. Davies, J. Denhartog, J. W. Mayer, O. L. Marsh, and P. Mankarious, Appl. Phys. Lett. 10, 323 (1967).
[112]J. A. Cairns and R. S. Nelson, Phys. Lett. A27, 14 (1968).
[113]E. Bøgh, in Interaction of Radiation with Solids, Ed. A. Bishay, N. Y., Plenum Press, 1967, p. 361.
[114]E. Uggerhoj and J. U. Andersen, Can. J. Phys. 46, 543 (1967).
[115]G. Fladda, P. Mazzoldi, E. Rimini, D. Sigurd, and L. Eriksson, Radiat. Eff. 1, 249 (1969).
[116]J. W. Mayer, J. A. Davies, and L. Eriksson, Appl. Phys. Lett. 11, 365 (1967).
[117]V. A. Somenkov, A. V. Gurskaya, M. G. Zemlyakov, M. E. Kost, N. A. Chernoplekov, and A. A. Chertkov, Fiz. Tverd. Tela 10, 1076 (1968) [Sov. Phys. Solid State 10, 852 (1968)].
[118]R. B. Alexander, P. T. Callaghan, and J. M. Poate, in Abstracts of the Intern. Conf. on Ion Implantation, New York, 1972, p. 57.
[119]P. P. Matyash, N. A. Skakun, and N. P. Dikiĭ, ZhETF Pis. Red. 19, 31 (1974) [JETP Letters 19, 18 (1974)].
[120]V. V. Beloshitskiĭ, N. P. Dikiĭ, M. A. Kumakhov, P. P. Matyash, and N. A. Skakun, cited in ref. 54, p. 43.
[121]L. T. Chadderton, Phil. Mag. 18, 1017 (1968); J. Appl. Cryst. 3, 429 (1970).
[122]A. G. Kadmenskiĭ, G. A. Iferov, and A. F. Tulinov, cited in ref. 29, p. 45.
[123]O. B. Firsov, Radiat. Eff. 21, 265 (1974).

Translated by C. S. Robinson